Title 40 CFR Part 191
Subparts B and C
Compliance Recertification Application 2026
for the
Waste Isolation Pilot Plant

Appendix PA-2026
Attachment A: Final State Analysis

United States Department of Energy
Waste Isolation Pilot Plant

Carlsbad Field Office
Carlsbad, New Mexico

Appendix PA-2026
Attachment A: Final State Analysis

TABLE OF CONTENTS

PA-A-1.0 INTRODUCTION 1

PA-A-2.0 DIFFERENCES BETWEEN THE IS AND FS PAS 3
PA-A-2.1 Computational Grid 3
PA-A-2.2 Waste Inventory 4
PA-A-2.3 Parameter Updates 5
PA-A-2.4 Culebra Release Points 6

PA-A-3.0 OVERVIEW OF FS PA METHODOLOGY 8

PA-A-4.0 RESULTS FOR THE UNDISTURBED REPOSITORY 9
PA-A-4.1 Fluid Flow in the Salado 9
PA-A-4.2 Radionuclide Transport in the Salado 14
PA-A-4.3 Radionuclide Transport in the Shaft 14

PA-A-5.0 RESULTS FOR A DISTURBED REPOSITORY 15
PA-A-5.1 Fluid Flow 15
PA-A-5.1.1 Fluid Flow in the Salado for E1 Intrusion Scenarios 15
PA-A-5.1.2 Fluid Flow in the Salado for E2 Intrusion Scenarios 21
PA-A-5.1.3 Summary of Fluid Flow in the Salado 26
PA-A-5.1.4 Fluid Flow in the Culebra 29
PA-A-5.2 Radionuclide Transport 30
PA-A-5.2.1 Mobilized Radionuclide Concentrations 30
PA-A-5.2.2 Transport through MBs and Shaft 31
PA-A-5.2.3 Transport to the Culebra 31
PA-A-5.2.4 Transport through the Culebra 34
PA-A-5.3 Direct Releases 36
PA-A-5.3.1 Cuttings and Cavings 37
PA-A-5.3.2 Spallings 37
PA-A-5.3.3 Direct Brine Releases 42

PA-A-6.0 NORMALIZED RELEASES 45
PA-A-6.1 Cuttings and Cavings 45
PA-A-6.2 Spallings 46
PA-A-6.3 Direct Brine 47
PA-A-6.4 Groundwater Transport 48
PA-A-6.5 Total Normalized Releases 49
PA-A-6.6 Parameter Sensitivity Analysis 53

PA-A-7.0 REFERENCES 55

LIST OF FIGURES

Figure PA-A-1. Final State Repository Layout 2
Figure PA-A-2. Salado Flow and Transport Grid for the CRA26_FS with Modeled Area Descriptions 4
Figure PA-A-3. Culebra Release Point Locations 7
Figure PA-A-4. Minimum, Maximum, and Mean of WP Pressure, Scenario S1-BF 10
Figure PA-A-5. Minimum, Maximum, and Mean of SROR Pressure, Scenario S1-BF 10
Figure PA-A-6. Minimum, Maximum, and Mean of NROR Pressure, Scenario S1-BF 11
Figure PA-A-7. Minimum, Maximum, and Mean of WROR Pressure, Scenario S1-BF 11
Figure PA-A-8. Minimum, Maximum, and Mean of WP Brine Saturation, Scenario S1-BF 12
Figure PA-A-9. Minimum, Maximum, and Mean of SROR Brine Saturation, Scenario S1-BF 12
Figure PA-A-10. Minimum, Maximum, and Mean of NROR Brine Saturation, Scenario S1-BF 13
Figure PA-A-11. Minimum, Maximum, and Mean of WROR Brine Saturation, Scenario S1-BF 13
Figure PA-A-12. Minimum, Maximum, and Mean of Brine Flow up the Shaft, Scenario S1-BF 14
Figure PA-A-13. Minimum, Maximum, and Mean of WP Pressure, Scenario S2-BF 16
Figure PA-A-14. Minimum, Maximum, and Mean of SROR Pressure, Scenario S2-BF 17
Figure PA-A-15. Minimum, Maximum, and Mean of NROR Pressure, Scenario S2-BF 17
Figure PA-A-16. Minimum, Maximum, and Mean of WROR Pressure, Scenario S2-BF 18
Figure PA-A-17. Minimum, Maximum, and Mean of WP Brine Saturation, Scenario S2-BF 18
Figure PA-A-18. Minimum, Maximum, and Mean of SROR Brine Saturation, Scenario S2-BF 19
Figure PA-A-19. Minimum, Maximum, and Mean of NROR Brine Saturation, Scenario S2-BF 19
Figure PA-A-20. Minimum, Maximum, and Mean of WROR Brine Saturation, Scenario S2-BF 20
Figure PA-A-21. Minimum, Maximum, and Mean Cumulative Brine Flow up the Borehole, Scenario S2-BF 20
Figure PA-A-22. Minimum, Maximum, and Mean of WP Pressure, Scenario S4-BF 22
Figure PA-A-23. Minimum, Maximum, and Mean of SROR Pressure, Scenario S4-BF 22
Figure PA-A-24. Minimum, Maximum, and Mean of NROR Pressure, Scenario S4-BF 23
Figure PA-A-25. Minimum, Maximum, and Mean of WROR Pressure, Scenario S4-BF 23
Figure PA-A-26. Minimum, Maximum, and Mean of WP Brine Saturation, Scenario S4-BF 24
Figure PA-A-27. Minimum, Maximum, and Mean of SROR Brine Saturation, Scenario S4-BF 24
Figure PA-A-28. Minimum, Maximum, and Mean of NROR Brine Saturation, Scenario S4-BF 25
Figure PA-A-29. Minimum, Maximum, and Mean of WROR Brine Saturation, Scenario S4-BF 25
Figure PA-A-30. Minimum, Maximum, and Mean Cumulative Brine Flow up the Borehole, Scenario S4-BF 26
Figure PA-A-31. Ensemble Mean Flow Rates 30
Figure PA-A-32. Mean Mobilized Radionuclide Concentrations Vs Time. Castile (ERDA-6) Brine 31
Figure PA-A-33. Cumulative Brine Releases up the Borehole 33
Figure PA-A-34. Cumulative Lumped Radionuclide Release[1] 34
Figure PA-A-35. Exceedance Probability of Cumulative Mass to the LWB in 10,000 Years for Full Mining Scenario 35
Figure PA-A-36. Exceedance Probability of Cumulative Mass to the LWB in 10,000 Years for Partial Mining Scenario 36
Figure PA-A-37. Non-Zero Spallings Release Volume by Scenario 40
Figure PA-A-38. Non-Zero Spallings Release Volume by Location[2] 41
Figure PA-A-39. Spallings Release Concentration from Closure to 10,000 Years 41
Figure PA-A-40. DBR Volume Frequency, All Intrusions 44
Figure PA-A-41. DBR Volumes, All Non-Zero Releases[2] 44
Figure PA-A-42. Overall Mean Cuttings and Cavings Releases 46

Figure PA-A-43. Overall Mean Spallings Releases 47
Figure PA-A-44. Overall Mean Direct Brine Releases 48
Figure PA-A-45. Overall Mean Releases Through the Culebra 49
Figure PA-A-46. Total Releases for Replicate 1 of the CRA26_FS 50
Figure PA-A-47. Total Releases for Replicate 2 of the CRA26_FS 51
Figure PA-A-48. Total Releases for Replicate 3 of the CRA26_FS 51
Figure PA-A-49. Overall Mean Release Components for the CRA26_FS 52
Figure PA-A-50. Overall Mean Total Releases for the CRA26_FS 52

LIST OF TABLES

Table PA-A-1. Inventory Iron, CPR, and Decay Heat Concentrations 5
Table PA-A-2. Updated Parameters for the CRA26_FS 6
Table PA-A-3. Pressure (MPa) Statistics on Replicate 1 Means 27
Table PA-A-4. Brine Saturation Statistics on Replicate 1 Means 28
Table PA-A-5. Brine Flow (m^3) Statistics for Replicate 1 29
Table PA-A-6. Caving Area Statistics for CRA26_FS and CRA26_IS 37
Table PA-A-7. Spallings Volume Summary for Replicate 1 39
Table PA-A-8. DBR Volume Statistics 43
Table PA-A-9. Statistics on the Overall Mean for Total Releases 53

ACRONYMS AND ABBREVIATIONS

%	percent
CCDF	complementary cumulative distribution function
CFR	Code of Federal Regulations
CH-TRU	contact-handled transuranic
Ci	curies
CI	confidence interval
CPR	cellulosic, plastic, and rubber
CRA	Compliance Recertification Application
DBR	direct brine release
E	deep drilling scenario
EPA	U.S. Environmental Protection Agency
ERDA	U.S. Energy Research and Development Administration
EXP	experimental area
FVW	fraction of excavated repository volume occupied by waste
GWB	Generic Weep Brine
kg	kilogram
L	liter
LWB	Land Withdrawal Boundary
M	mining scenario
m	meter
m^2	square meters
m^3	cubic meters
MB	marker bed
ME	mining and drilling scenario
mol	mole
MPa	megapascal
NROR	North Rest-of-Repository
Pa	Pascal
PA	performance assessment
RPPCR	Replacement Panels Planned Change Request

s	second
s^2	seconds squared
SROR	South Rest-of-Repository
TRU	transuranic
WIPP	Waste Isolation Pilot Plant
WOP	West Operations Area
WP	waste panel
WROR	West Rest-of-Repository

ELEMENTS AND CHEMICAL COMPOUNDS

Am	americium
$C_6H_{10}O_5$	generic formula for CPR
Fe	iron
H_2	hydrogen gas
Mg	magnesium
MgO	magnesium oxide, or periclase
Np	neptunium
Pu	plutonium
Th	thorium
U	uranium

PA-A-1.0 Introduction

Appendix PA of the 2026 Compliance Recertification Application (CRA-2026) documents the performance assessment (PA) conducted for the Interim State (IS) repository configuration, which consists of 12 waste panels (10 original panels and 2 replacement panels). The IS repository configuration is regarded as an interim state because it does not provide sufficient volume for disposal of the full allowable waste volume designated for the Waste Isolation Pilot Plant (WIPP) under the Land Withdrawal Act (LWA) (U.S. Congress 1996).

This attachment supplements Appendix PA by documenting a PA conducted for the Final State (FS) repository configuration. The FS repository configuration consists of 19 waste panels, including 10 original panels, 2 replacement panels, and 7 additional panels located to the west of the existing operations area. The additional panels are denoted as Panels 13 through 19. Figure PA-A-1 illustrates the layout of the FS repository, highlighting the locations of the original, replacement, and additional panels.

The FS repository design provides sufficient volume to accommodate the full allowable waste volume designated for WIPP under the LWA (U.S. Congress 1996). The FS repository configuration is evaluated to assess the potential impacts of this expanded footprint and increased waste inventory on repository performance. Although the FS repository design represents the best estimate of the final configuration needed to dispose of the full LWA waste volume, the seven additional panels have not yet been approved for disposal of transuranic (TRU) waste.

This attachment documents the differences between the IS and FS PAs and presents the results of the FS PA. The FS PA builds upon the methodology and process models used in the IS PA, with updates to account for changes associated with the FS repository configuration. The results presented in this attachment demonstrate that the FS repository remains in compliance with the containment requirements of 40 CFR Part 191.

In this attachment, the PA for the 12-panel Interim State repository configuration documented in Appendix PA of the CRA-2026 is referred to as CRA26_IS (Hansen et al. 2025). The PA for the 19-panel Final State repository configuration evaluated in this attachment is referred to as CRA26_FS (Zeitler et al. 2025).

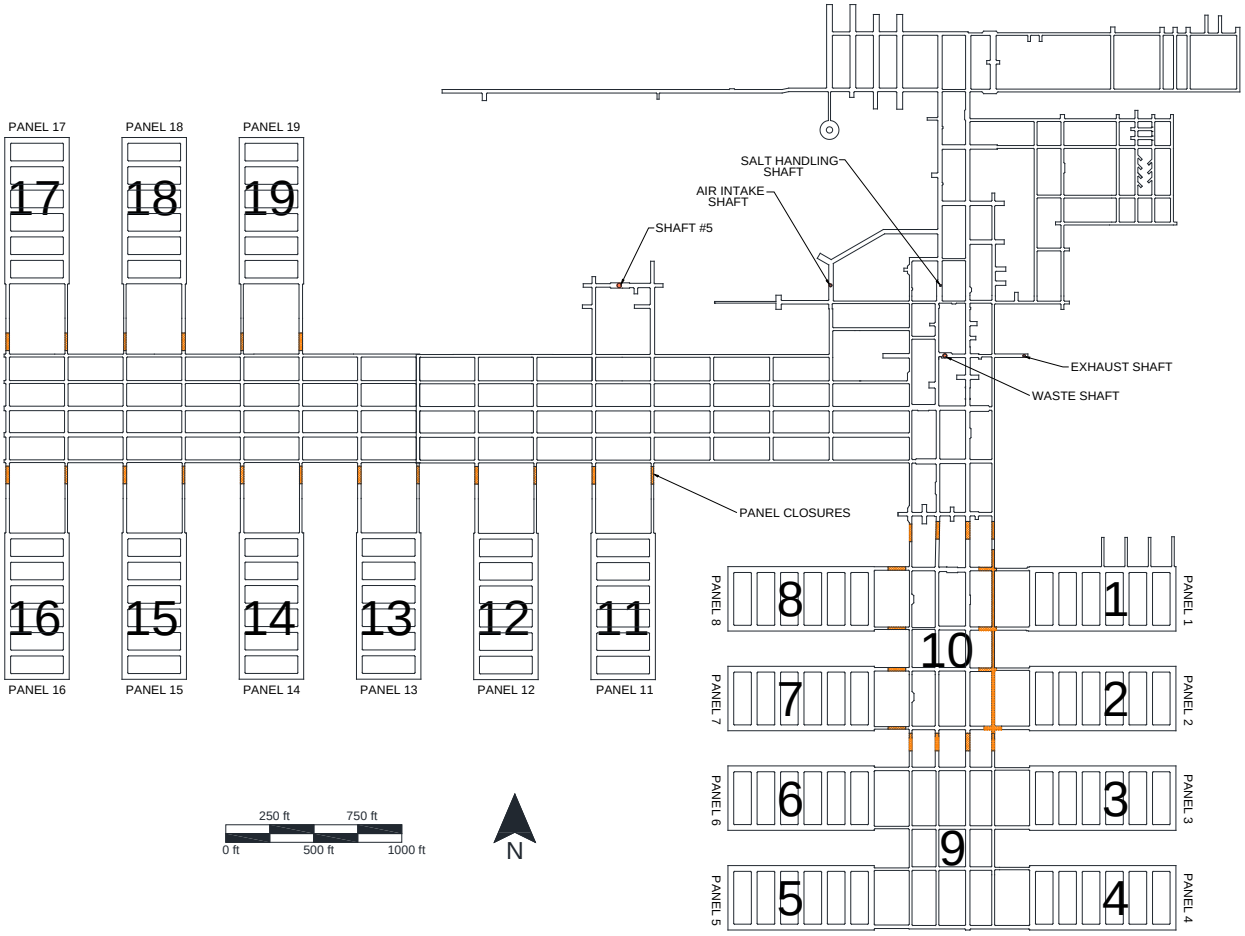


Figure PA-A-1. Final State Repository Layout

PA-A-2.0 Differences Between the IS and FS PAs

The PA for the FS repository differs from the CRA-2026 PA for the IS repository in the following ways:

1. Computational grid: The Salado flow and transport computational grid is modified to reflect the FS repository design.
2. Waste inventory: Waste inventory scaling and radionuclide concentrations are adjusted to be consistent with the FS repository's increased volume.
3. Parameter updates: Parameters are updated to account for changes in repository area and volume, baseline actinide solubilities, humic colloidal enhancement parameters, and minimum brine volume for direct brine releases.
4. Release points into Culebra Dolomite Member of the Rustler Formation (Culebra): Two additional Culebra release points (CRPs) are included to account for the additional waste panels.

PA-A-2.1 Computational Grid

The transition from the IS repository configuration to the FS repository configuration requires modifications to the computational grid used for Salado flow and transport modeling. These modifications are required to represent the expanded repository footprint and increased waste storage volume associated with the FS repository configuration. The Salado flow and transport computational grid is used by the BRAGFLO and NUTS codes to simulate brine and gas flow and radionuclide transport in the Salado Formation.

Changes to the computational grid include:

1. Grid dimensions: Grid spacing and boundaries are adjusted to represent the additional waste panels (Day 2025). These adjustments include adding volume to the West Rest-of-Repository to account for Panels 13 through 19, adding volume to the West Drifts to represent the drifts extending to the additional panels, and adding volume to the Run-of-Mine Salt Panel Closure separating the West Drifts from the West Rest-of-Repository.
2. Far-field Salado representation: The flaring of the far-field Salado is recalculated based on the updated grid dimensions. The distance to the North Land Withdrawal Boundary (LWB) is calculated as the minimum distance from the westernmost edge of the excavated repository to the nearest LWB to the west, and the distance to the South LWB is calculated as the minimum distance from the southernmost edge of the excavated repository to the nearest LWB to the south (Day 2025).

Figure PA-A-2 illustrates the BRAGFLO grid for the FS repository, highlighting the modeled area descriptions and cell dimensions.

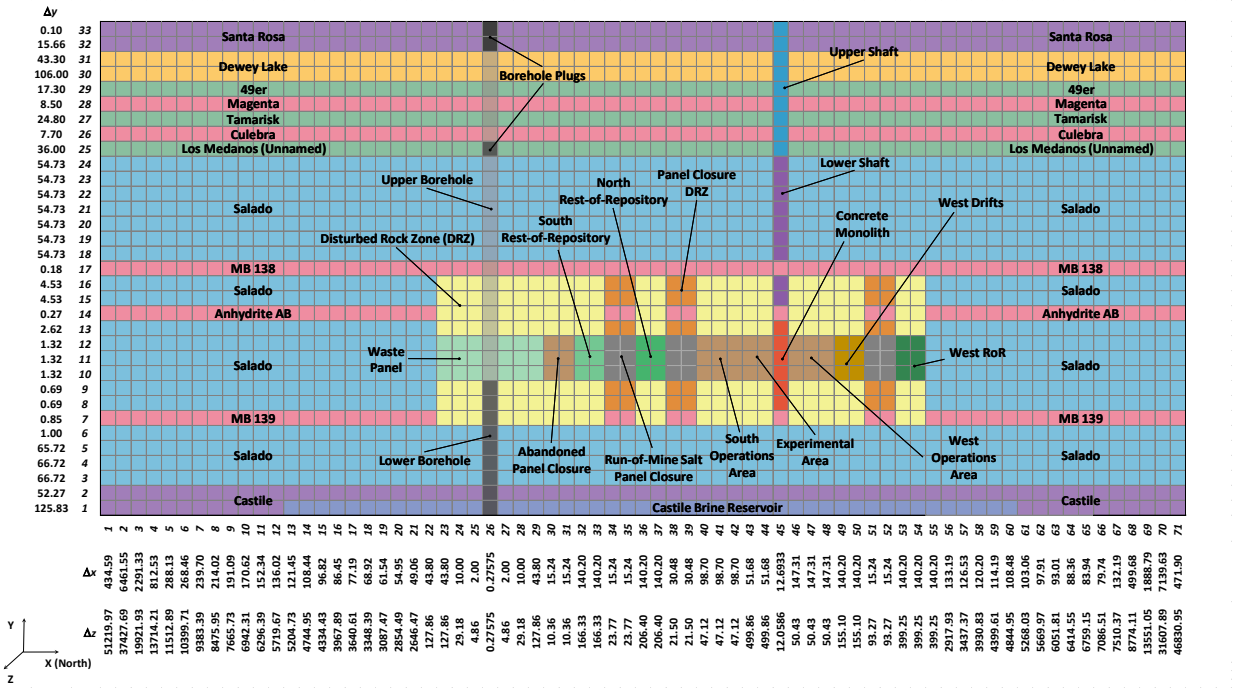


Figure PA-A-2. Salado Flow and Transport Grid for the CRA26_FS with Modeled Area Descriptions.

PA-A-2.2 Waste Inventory

For the FS repository, the waste volume is set to the statutory limit established by the LWA (U.S. Congress 1996). The waste inventory for the FS repository is described in the Full Repository Performance Assessment Inventory Report – 2024 (Van Soest 2025a).

Key differences between the waste inventories for the IS and FS repository configurations include:

1. Total waste volume: The waste volume increases from 157,837.92 cubic meters (m^3) (IS repository) to 175,564 m^3 (FS repository) to align with the LWA limit (Van Soest 2025a; Ward 2025).

2. Inventory concentrations (normalized to repository volume)**:** Relative to the IS repository, the FS repository exhibits lower concentrations of iron, cellulosics, plastics, and rubber (CPR), as well as lower decay heat, due to distribution of the waste inventory over the larger repository volume (Zeitler et al. 2025).

3. Radionuclide activity: The total activity of the FS repository inventory at closure is 9.68 × 10^6 Curies (Ci), compared to 8.05 × 10^6 Ci for the IS repository inventory (Kicker 2025a; Kicker 2025b). The increase is primarily due to scaling of waste with long-lived radionuclides to the statutory waste volume.

Table PA-A-1 compares key aspects of the IS and FS inventories, normalized by the waste storage volume of each repository.

Table PA-A-1. Inventory Iron, CPR, and Decay Heat Concentrations

Input	Unit	CRA26_IS Value	CRA26_FS Value	CRA26_FS to CRA26_IS Ratio
Iron	kg/m³	126.83	97.93	0.77
CPR	kg/m³	40.48	29.09	0.72
Decay Heat	watt/m³	0.43	0.31	0.73

PA-A-2.3 Parameter Updates

The FS repository configuration requires updates to several repository parameters to account for the expanded footprint and increased waste inventory. These parameter updates include:

1. Repository dimensions: Parameters describing repository dimensions are updated to reflect the expanded footprint and increased waste storage volume of the FS repository.
2. Minimum brine volume for Direct Brine Releases (DBRs) (GLOBAL:DBRMINBV): The minimum brine volume for a DBR was increased from 6,314 m³ in the IS repository to 9,608 m³ in the FS repository (Brunell 2025). The increase reflects the larger repository footprint. This volume is used to compute baseline actinide solubilities.
3. Humic colloidal parameters: Proportionality constants for humic colloids are reevaluated based on updates to the baseline solubility values. Updated values for radionuclides in the +III and +IV oxidation states are defined by Mariner (2025).
4. Inventory Parameters: As discussed in Section PA-A-2.2, updated waste inventory parameters are defined based on the inventory specified in Van Soest (2025a) and documented by Kicker (2025a).
5. Baseline actinide solubilities: Baseline solubilities for actinides in the +III, +IV, and +V oxidation states in Generic Weep Brine (GWB) and U.S. Energy Research and Development Administration Well 6 (ERDA-6) brines are computed for the FS repository inventory and minimum brine volume. Actinide solubilities for the FS repository are generally lower than those for the IS repository due to decreased organic ligand concentrations (Domski 2025).

Table PA-A-2 lists updated parameter values used in the CRA26_FS analysis. A complete list of parameters used in the CRA26_FS is provided in Feng and Kicker (2025).

Table PA-A-2. Updated Parameters for the CRA26_FS

Material	Property	Description	CRA26_IS Value	CRA26_FS Value	Units
REFCON	VREPOS	Excavated storage volume of repository.	560,722.29	905,734.49	m^3
REFCON	ABERM	Area of Berm Placed Over Waste Panels.	750,000	1,268,303	m^2
REFCON	AREA_CH	Area For CH Waste Disposal.	141,511	228,582	m^2
REFCON	FVW	Fraction of Repository Volume Occupied by Waste.	0.279	0.186	-
REFCON	AREA_RH	Area For RH Waste Disposal.	3,528	15,760	m^2
GLOBAL	DBRMINBV	Minimum volume of brine in the repository required for a direct brine release.	6,314	9,608	m^3
PHUMOX3	PHUMCIM	Proportionality constant with humic colloids for actinides with oxidation state III in Castile brine.	0.3	0.4	-
PHUMOX4	PHUMSIM	Proportionality constant with humic colloids for actinides with oxidation state IV in Salado brine.	0.02	0.01	-
BOREHOLE	WUF	Unit of Waste.	7.37	8.68	-
Various	Inventory	Inventory parameters defined in Appendix D of Kicker (2025a).	-	See Kicker (2025a), Appendix D.	-
SOLMOD (3/4/5)	SOL(C/S)OH (_/2/3/4/5)	Baseline Actinide Solubilities for actinides in the III, IV, and V oxidation states in Castile and Salado brines in 1x, 2x, 3x, 4x, and 5x minimum brine volumes as defined in Domski (2025).	-	See Domski (2025).	mol/L

PA-A-2.4 Culebra Release Points

The FS repository configuration includes four CRPs, compared to two in the IS repository configuration, as shown in Figure PA-A-3. CRP 3 and CRP 4 represent radionuclide releases from the westernmost waste panels (Panels 14 through 19).

In the CRA26_FS PA, CRP 2 represents releases from Panels 11, 12, and 13. In the IS PA, CRP 2 represents releases from Panels 11 and 12 only. The modeled location coordinates of CRP 2 are identical between the IS and FS analyses (Wilgus and Brunell 2025).

Figure PA-A-3 illustrates the locations of the CRPs for the FS repository configuration.

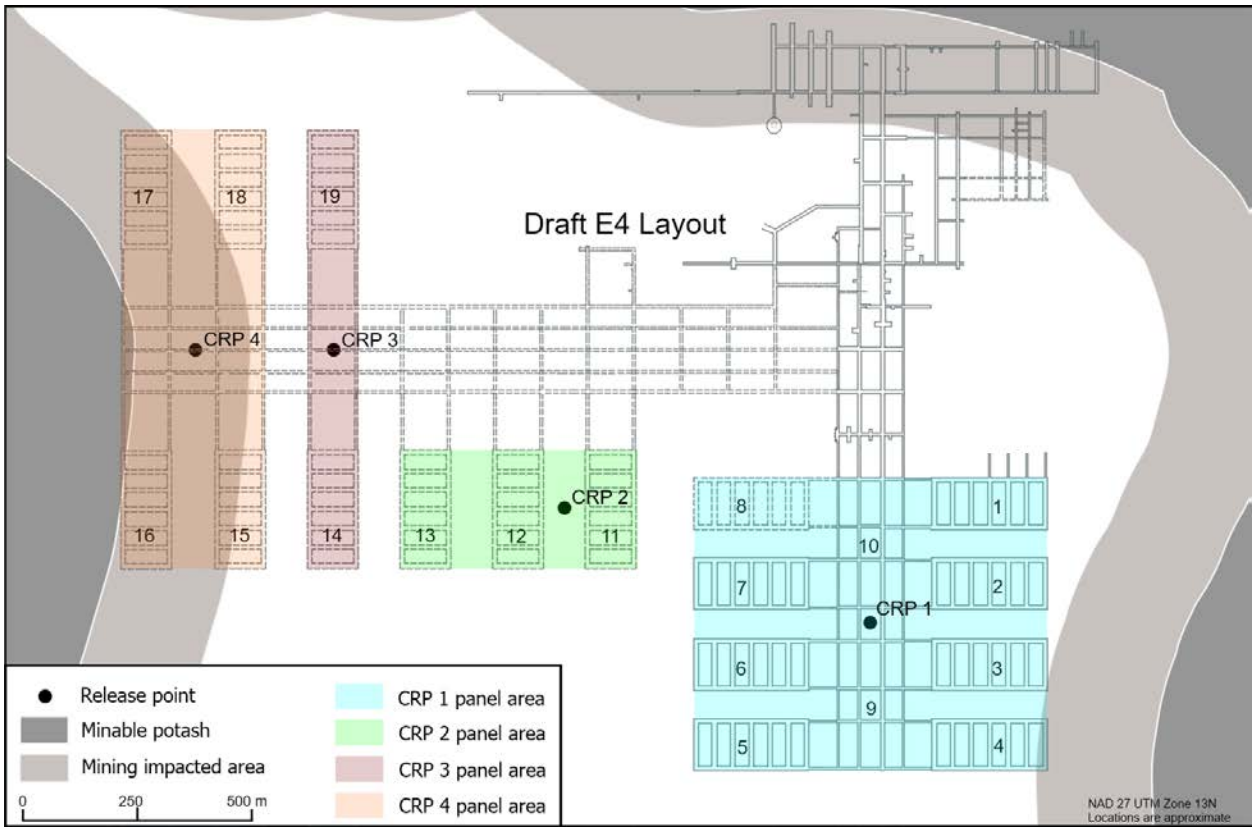


Figure PA-A-3. Culebra Release Point Locations

PA-A-3.0 Overview of FS PA Methodology

The PA for the FS repository configuration is conducted using the same methodology, process models, scenario definitions, screening approach, and treatment of uncertainty as the IS PA documented in Appendix PA. Accordingly, the CRA26_FS uses the same scenario framework as the CRA26_IS; scenario definitions for undisturbed and disturbed repository performance are provided in Appendix PA, Sections PA-2.2.2 and PA-3.4, while process-model-specific scenario implementations are described in the relevant computational sections of Appendix PA, including BRAGFLO scenarios (Section PA-6.3.1), spallings/DBR scenarios (Section PA-6.3.5), and Culebra flow and transport scenarios (Sections PA-6.3.7 and PA-6.3.8). No new conceptual models or release mechanisms are introduced for the FS analysis.

The FS PA applies the IS PA framework to an expanded repository footprint and panel layout. The changes described in Section PA-A-2.0 require revised panel neighbor assignments (Hansen et al. 2025) and the addition of two CRP to represent radionuclide transport pathways from the westernmost panels. The same Latin Hypercube Sampling design and sampled input parameter distributions are used for both the IS and FS calculations.

Two additional sets of SECOTP2D simulations are performed to support radionuclide transport modeling from the new CRPs. All other computational procedures, codes, and execution methods are unchanged from those used in the IS PA. Execution of the CRA26_FS PA calculations and archiving of results are documented in Long (2025).

PA-A-4.0 Results for the Undisturbed Repository

This section presents the PA results for the undisturbed repository in the FS configuration. The undisturbed repository scenario assumes no human intrusion or mining activities occur during the regulatory period of 10,000 years. Under these conditions, potential radionuclide releases are limited to transport through the Salado Formation and the repository shafts.

Overall, the undisturbed FS repository exhibits behavior consistent with that of the IS repository within the PA framework. As discussed in Section PA-A-4.1, repository pressures and brine flows for the FS configuration remain comparable to those of the IS configuration, despite differences in repository footprint and waste inventory. While brine saturations are generally higher in the FS case, these differences do not result in screened-in radionuclide transport pathways. As shown in Sections PA-A-4.2 and PA-A-4.3, radionuclide transport through the Salado Formation and the shafts remains negligible under undisturbed conditions for both configurations.

PA-A-4.1 Fluid Flow in the Salado

Figure PA-A-4 through Figure PA-A-7 compare minimum, maximum, and mean waste region pressures for scenario S1-BF, the undisturbed BRAGFLO scenario (Appendix PA, Section PA-6.3.1), between CRA26_FS and CRA26_IS. Statistics are assessed for the 100 vectors of Replicate 1; Replicates 2 and 3 exhibit similar behavior. Repository pressures increase over time due to rapid initial creep closure of rooms, initial inflow of brine leading to gas generation from corrosion and radiolysis, and the availability of CPR materials for microbial gas generation.

Several changes incorporated in the CRA26_FS (Section PA-A-2.0), in particular repository dimensions and waste inventory, influence repository pressurization. However, their effects are generally small (Zeitler et al. 2025). Mean pressures in the waste regions are similar to those observed in the CRA26_IS.

Brine saturations in the repository generally increase toward the south due to the one-degree southward dip of the Salado Formation and associated gravity-driven brine flow (Figure PA-A-8 through Figure PA-A-11). Compared to the CRA26_IS, brine saturations in the CRA26_FS are generally higher across waste regions for scenario S1-BF. These increases are attributed primarily to reduced brine consumption associated with lower inventory concentrations of activity, cellulose, and iron (Zeitler et al. 2025). Mean brine flows up the shaft for the CRA26_FS remain small over the regulatory period (Figure PA-A-12).

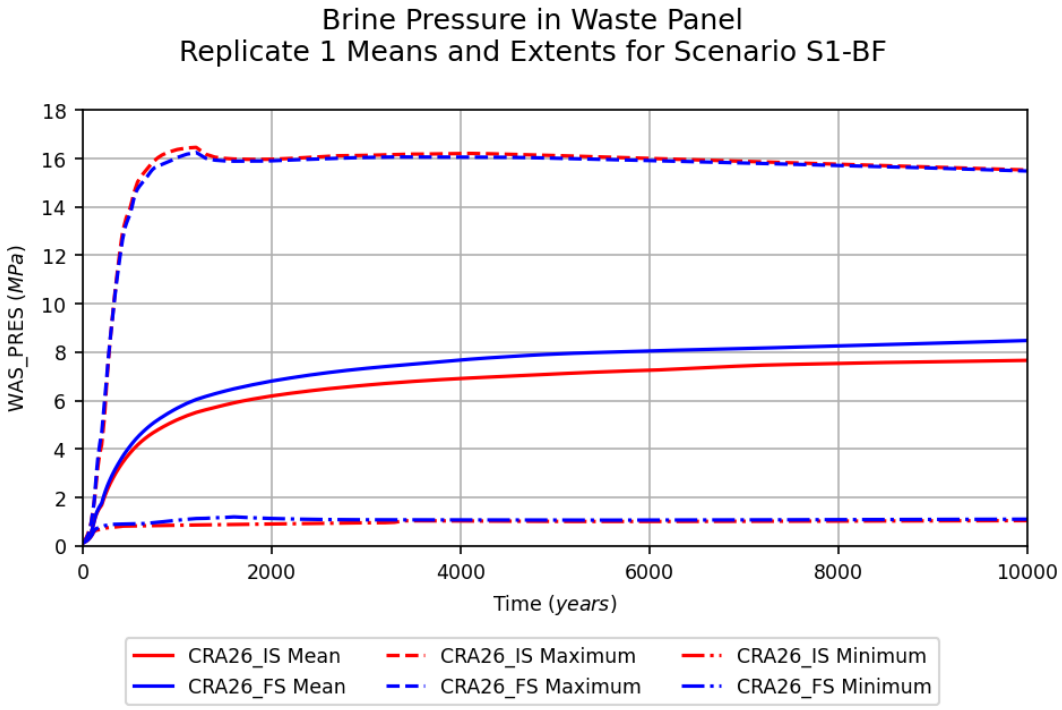


Figure PA-A-4. Minimum, Maximum, and Mean of WP Pressure, Scenario S1-BF

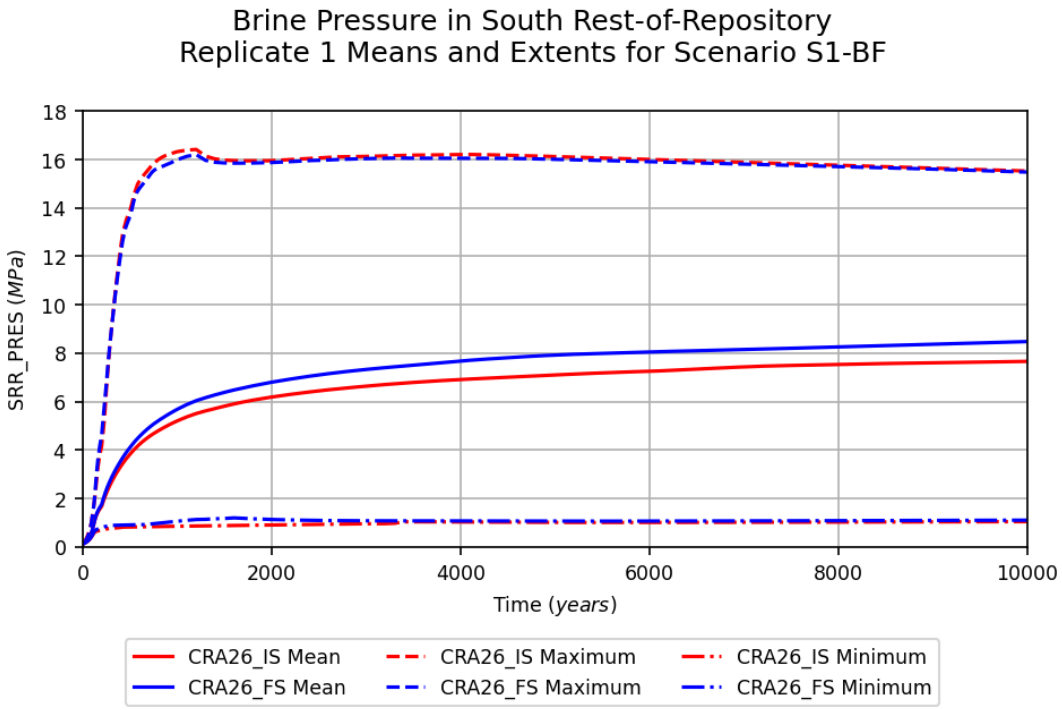


Figure PA-A-5. Minimum, Maximum, and Mean of SROR Pressure, Scenario S1-BF

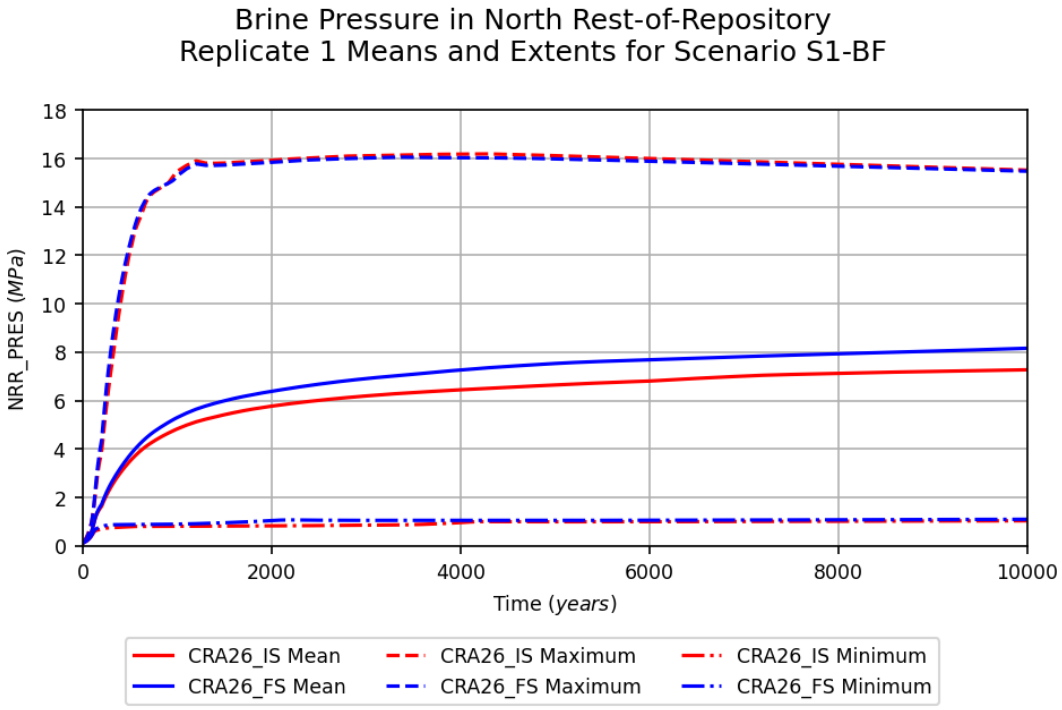


Figure PA-A-6. Minimum, Maximum, and Mean of NROR Pressure, Scenario S1-BF

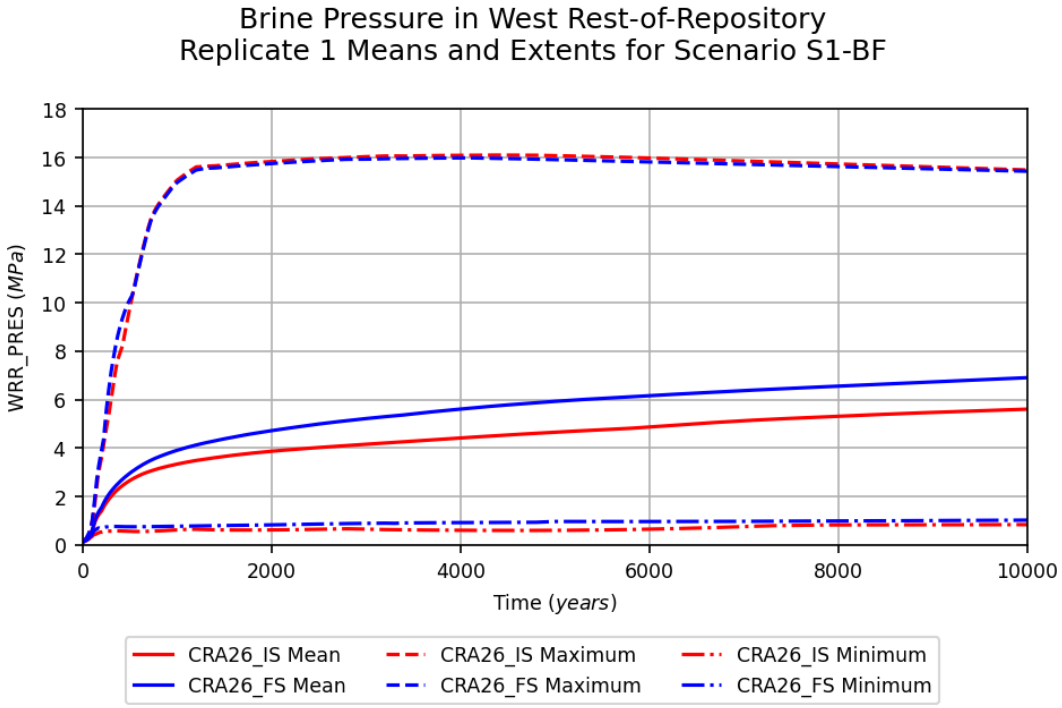


Figure PA-A-7. Minimum, Maximum, and Mean of WROR Pressure, Scenario S1-BF

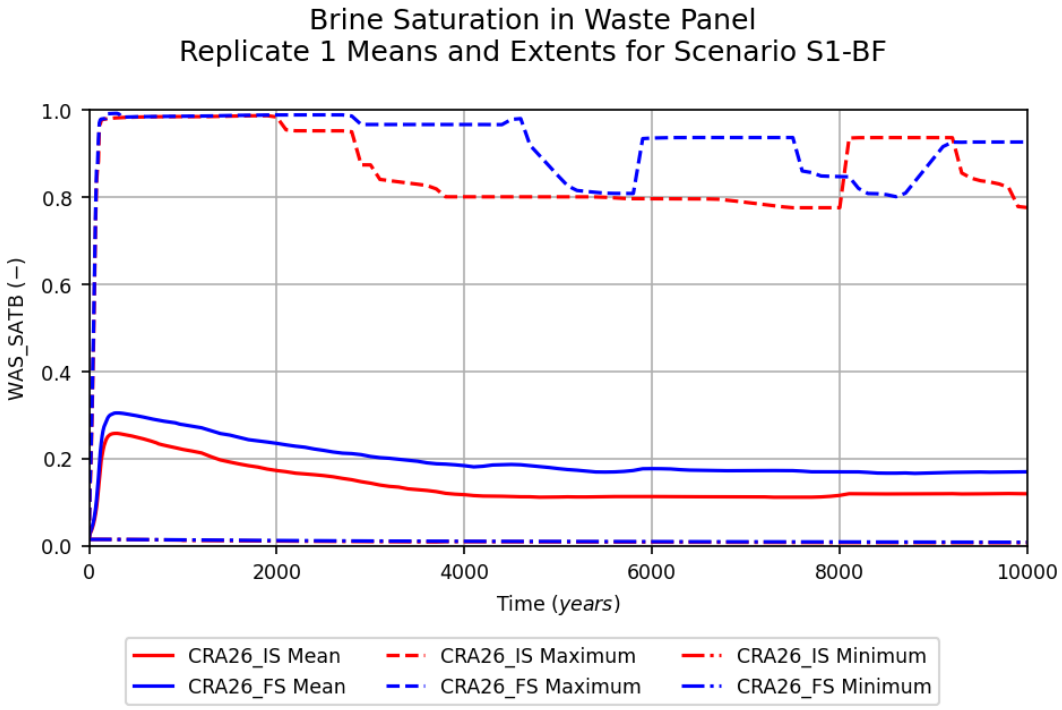


Figure PA-A-8. Minimum, Maximum, and Mean of WP Brine Saturation, Scenario S1-BF

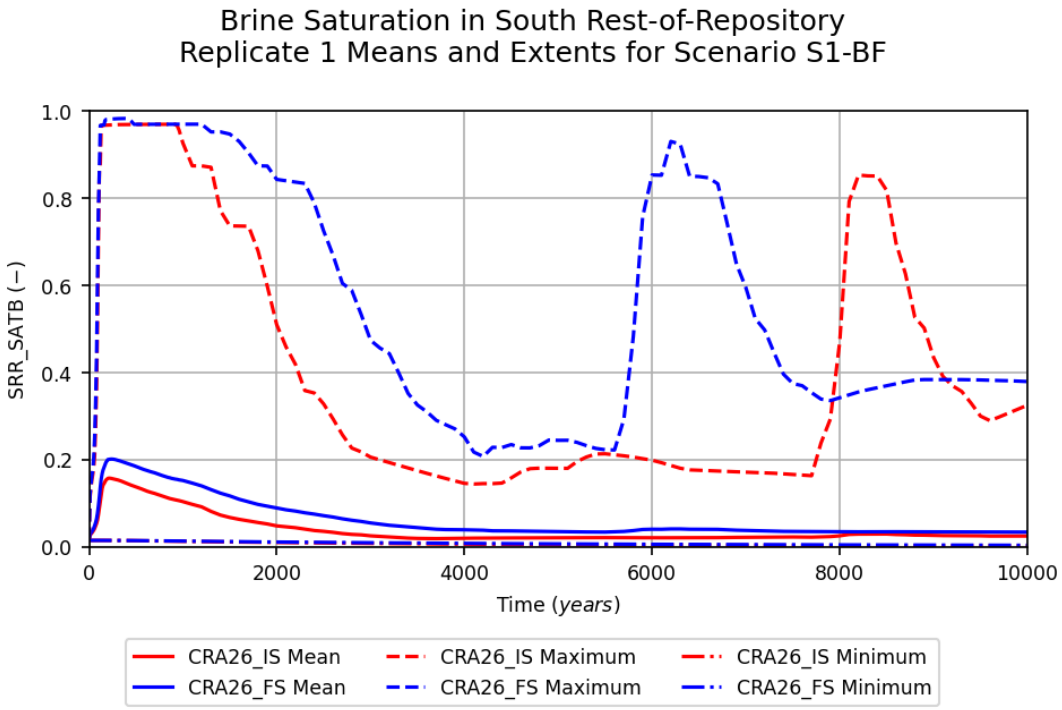


Figure PA-A-9. Minimum, Maximum, and Mean of SROR Brine Saturation, Scenario S1-BF

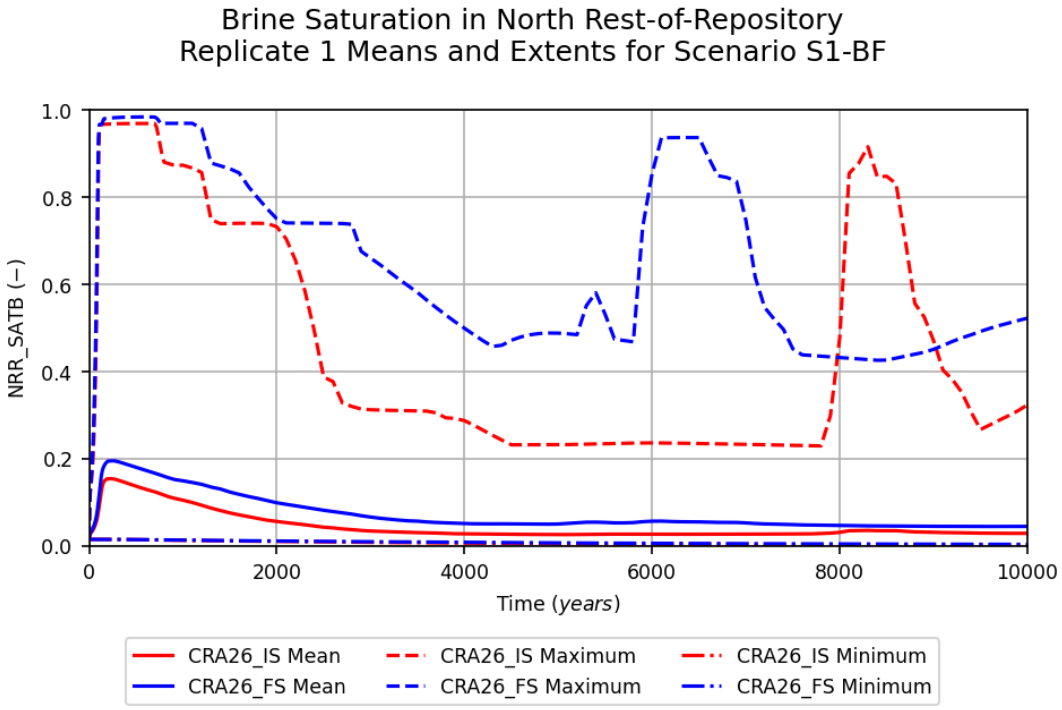


Figure PA-A-10. Minimum, Maximum, and Mean of NROR Brine Saturation, Scenario S1-BF

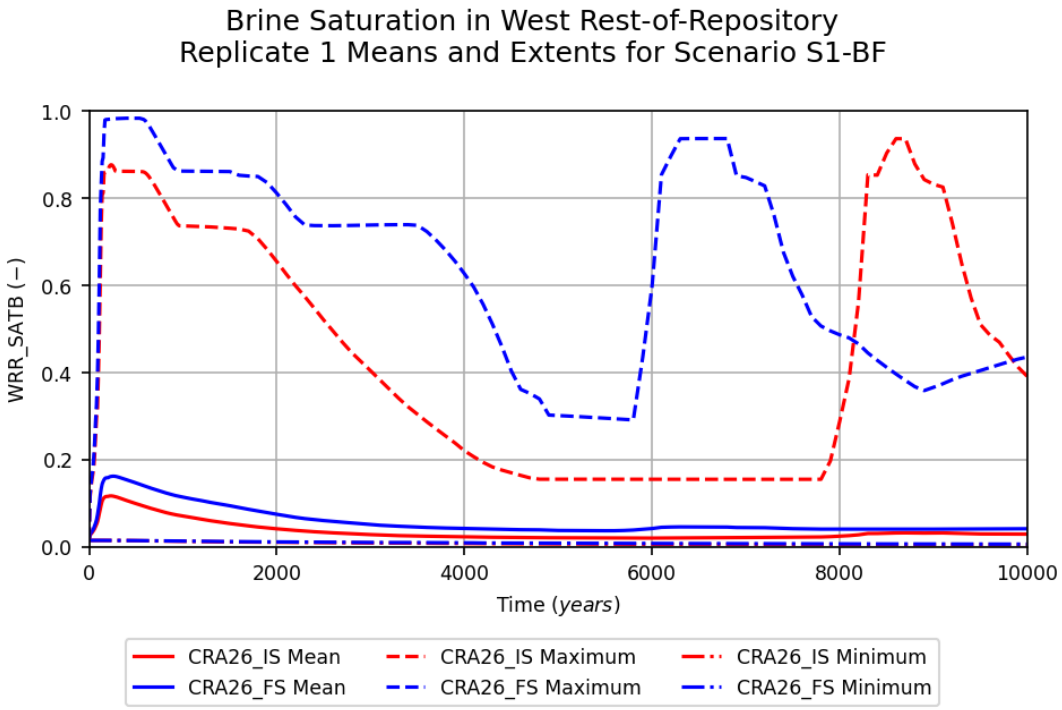


Figure PA-A-11. Minimum, Maximum, and Mean of WROR Brine Saturation, Scenario S1-BF

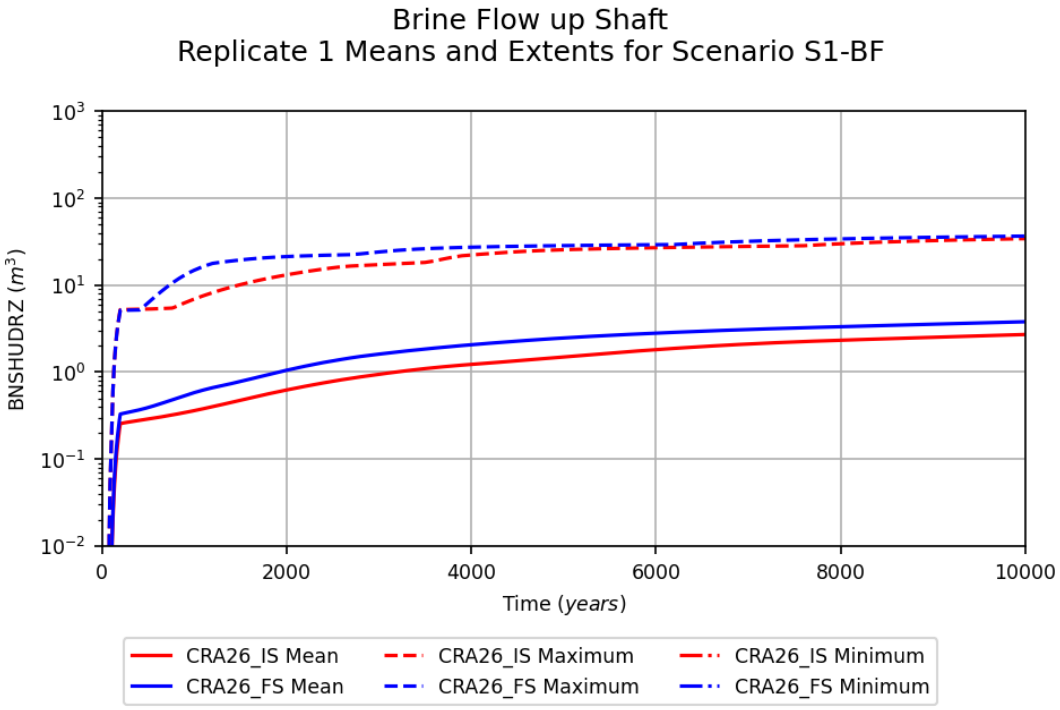


Figure PA-A-12. Minimum, Maximum, and Mean of Brine Flow up the Shaft, Scenario S1-BF

PA-A-4.2 Radionuclide Transport in the Salado

For the CRA26_FS, no vectors exceed the screening criterion for radionuclide transport through the Salado Formation to the accessible environment. This result is consistent with the CRA26_IS, which also demonstrated negligible radionuclide transport through the Salado under undisturbed conditions. The expanded repository footprint and increased waste inventory in the FS configuration did not alter the screening conclusions for Salado transport.

PA-A-4.3 Radionuclide Transport in the Shaft

Similar to the CRA26_IS, no vectors in the CRA26_FS showed radionuclide transport through the shafts to the Culebra. These results confirm that radionuclide transport through the shafts remains negligible under undisturbed conditions.

PA-A-5.0 Results for a Disturbed Repository

The WIPP repository might be disturbed by exploratory drilling for natural resources during the 10,000-year regulatory period. Drilling could create additional pathways for radionuclide transport through the Salado and could release material directly to the surface. In addition, mining for potash within the LWB might alter flow in the overlying geologic units and locally accelerate transport through the Culebra. The scenarios for disturbed repository performance capture the range of consequences resulting from drilling and mining, including releases from the repository and changes to the natural and repository system.

Total releases for disturbed scenarios comprise:

1. Transport Releases: Movement of radionuclides up an abandoned borehole into the Culebra, then through the Culebra to the LWB. Transport releases are influenced by the addition of CRP 3 and CRP 4 in the CRA26_FS, which account for radionuclide releases from the westernmost panels (Panels 14 through 19).

2. Direct Releases: Releases of solids (cuttings, cavings, and spallings) and brine-containing radionuclides (DBRs) at the time of a drilling intrusion. Direct releases are influenced by repository pressure and brine saturation. The CRA26_FS exhibits slightly higher brine pressures and saturations in some scenarios, leading to differences in direct release volumes compared to the CRA26_IS.

This section first summarizes the flow conditions in and around the repository that influence transport releases. Transport releases are presented next, followed by direct releases, i.e., cuttings, cavings, spallings, and DBRs. The CRA-2026 PA results obtained for the disturbed IS repository are summarized in Brunell et al. (2025). Process model results presented in this section are from Replicate 1, unless stated otherwise.

PA-A-5.1 Fluid Flow

This section summarizes the results for fluid flow in the Salado and Culebra for the disturbed scenarios. Fluid flow in the Salado is influenced by repository pressure, brine saturation, and the presence of drilling intrusions, while fluid flow in the Culebra is affected by transmissivity fields and mining scenarios. Fluid flow in the Salado is calculated by the BRAGFLO code (Appendix PA, Section PA-6.3.1) and flow in the Culebra using the MODFLOW6 code (Appendix PA, Section PA-6.3.7). Analyses of fluid flow in the Salado and Culebra are presented in Zeitler et al. (2025). Wilgus and Bethune (2025) present the Culebra flow results in detail.

PA-A-5.1.1 Fluid Flow in the Salado for E1 Intrusion Scenarios

E1 intrusion scenarios represent drilling events that intersect a waste-filled panel and also encounter a pressurized brine reservoir beneath the repository. Figure PA-A-13 through Figure PA-A-16 show the minimum, maximum, and mean pressures in the Waste Panel (WP), South Rest-of-Repository (SROR), North Rest-of-Repository (NROR), and West Rest-of-Repository

(WROR) regions for the CRA26_FS and compare to the CRA26_IS. The results show that pressures for S2-BF (Appendix PA, Section PA-6.3.1) are very similar between the CRA26_FS and CRA26_IS.

Figures PA-A-17 through PA-A-20 show the minimum, maximum, and mean brine saturations in the WP, SROR, NROR, and WROR for the CRA26_FS and compare to the CRA26_IS. Results for S2-BF scenarios indicate that brine saturations are generally increase in the CRA26_FS compared to the CRA26_IS. As with the undisturbed repository, the brine saturation increase in the waste areas may be attributed to the increase in repository footprint and the decreased brine consumption that results from lower concentrations of activity, cellulose, and iron (Zeitler et al. 2025).

Cumulative brine flows up the intrusion borehole potentially transport contaminants to the ground surface, or to the Culebra where contaminants may transport laterally through the Culebra to the LWB. Maximum and mean brine flows up the intrusion borehole to the Culebra obtained in the CRA26_FS and the CRA26_IS are plotted together in Figure PA-A-21. Note that minimum brine flows are zero and do not appear in Figure PA-A-21. Brine flow up the borehole for CRA26_FS is similar to the brine flow up the borehole for CRA26_IS.

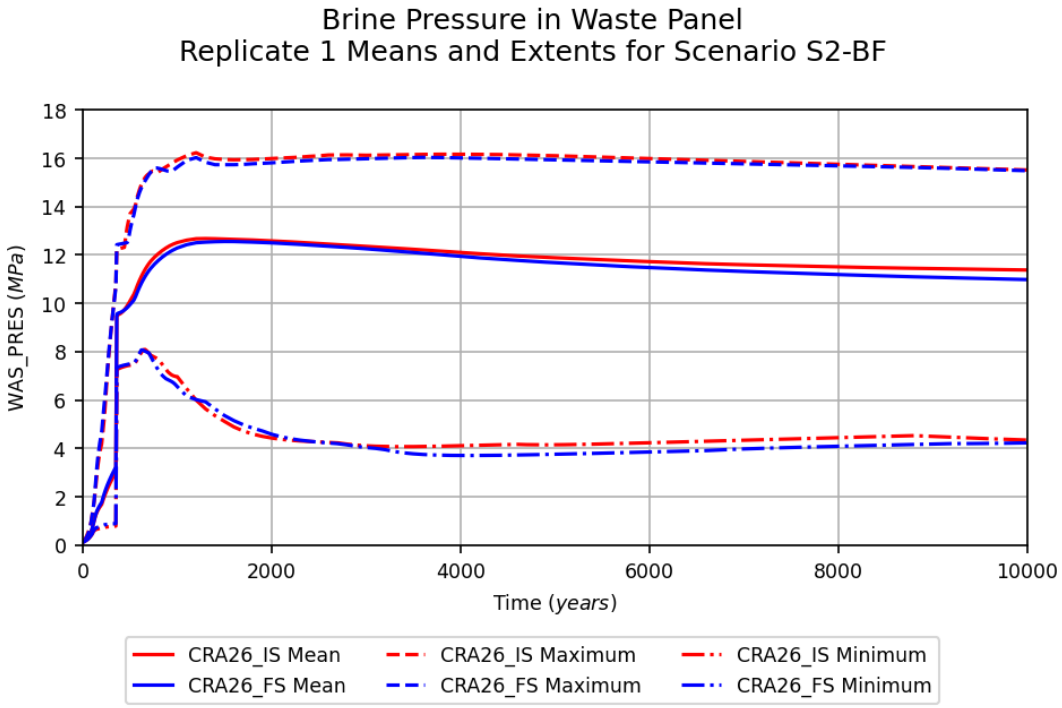


Figure PA-A-13. Minimum, Maximum, and Mean of WP Pressure, Scenario S2-BF

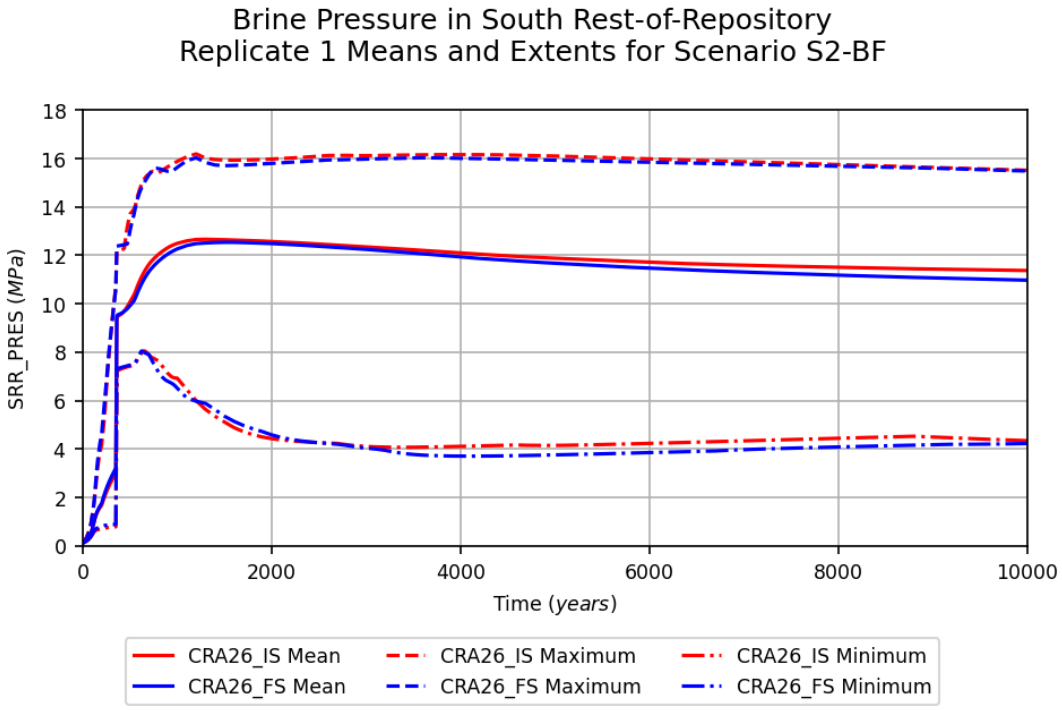


Figure PA-A-14. Minimum, Maximum, and Mean of SROR Pressure, Scenario S2-BF

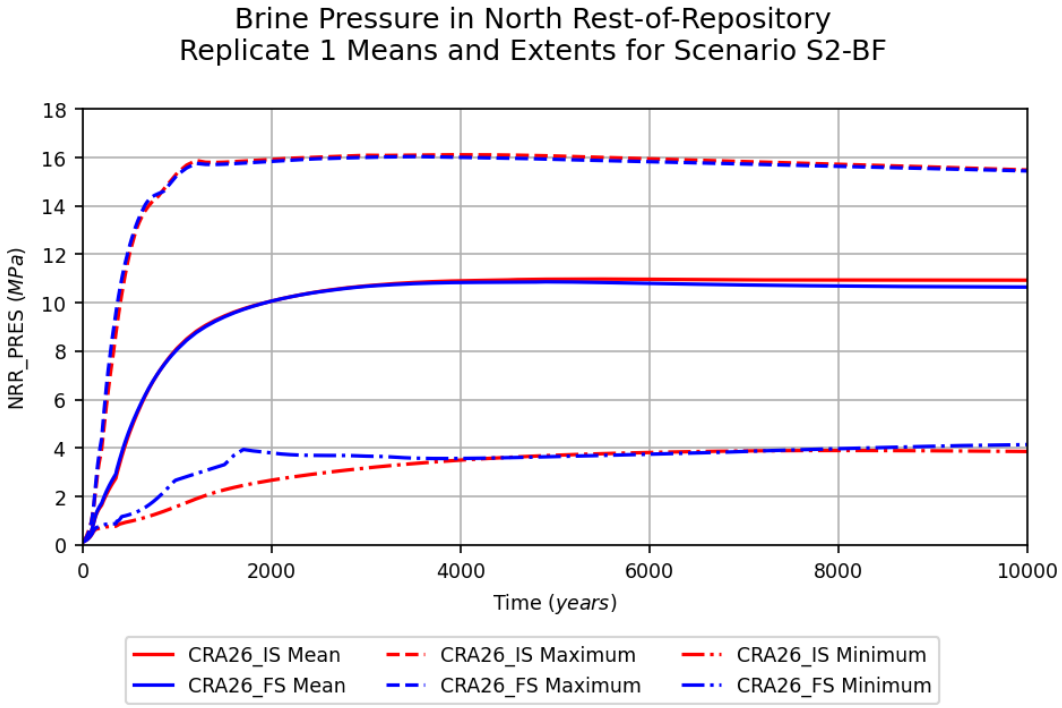


Figure PA-A-15. Minimum, Maximum, and Mean of NROR Pressure, Scenario S2-BF

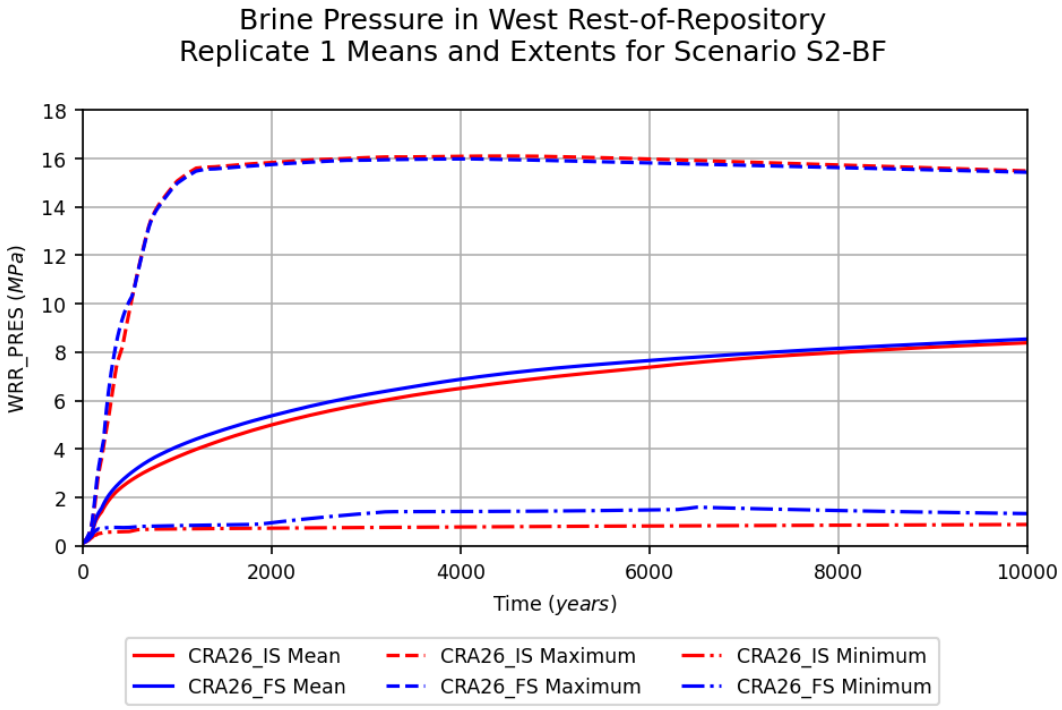


Figure PA-A-16. Minimum, Maximum, and Mean of WROR Pressure, Scenario S2-BF

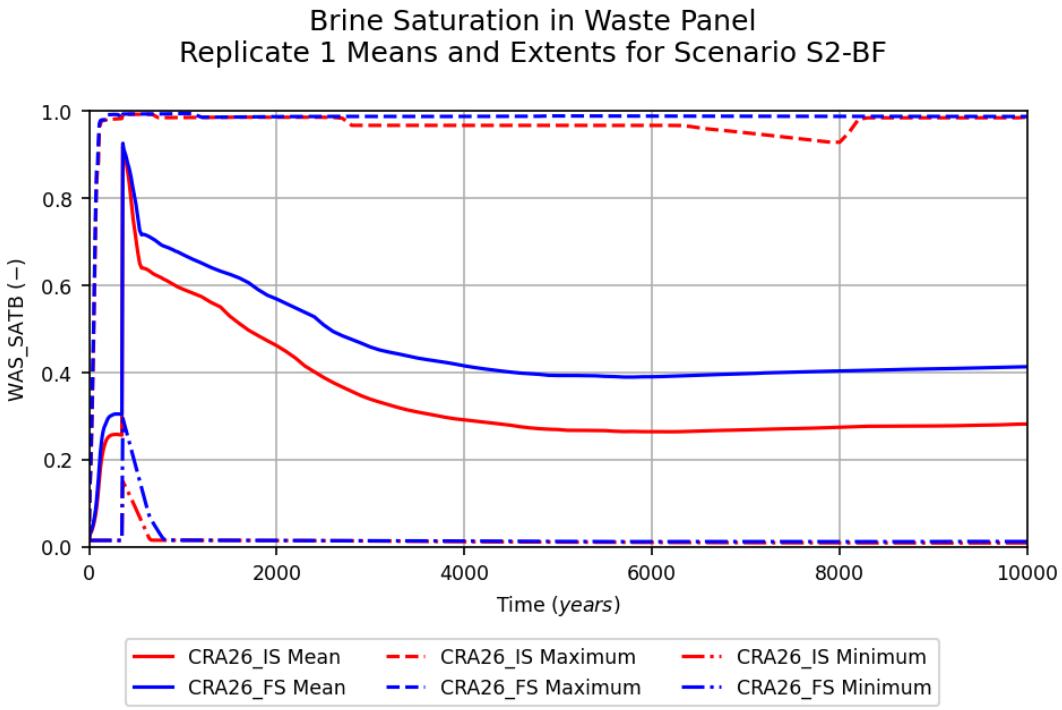


Figure PA-A-17. Minimum, Maximum, and Mean of WP Brine Saturation, Scenario S2-BF

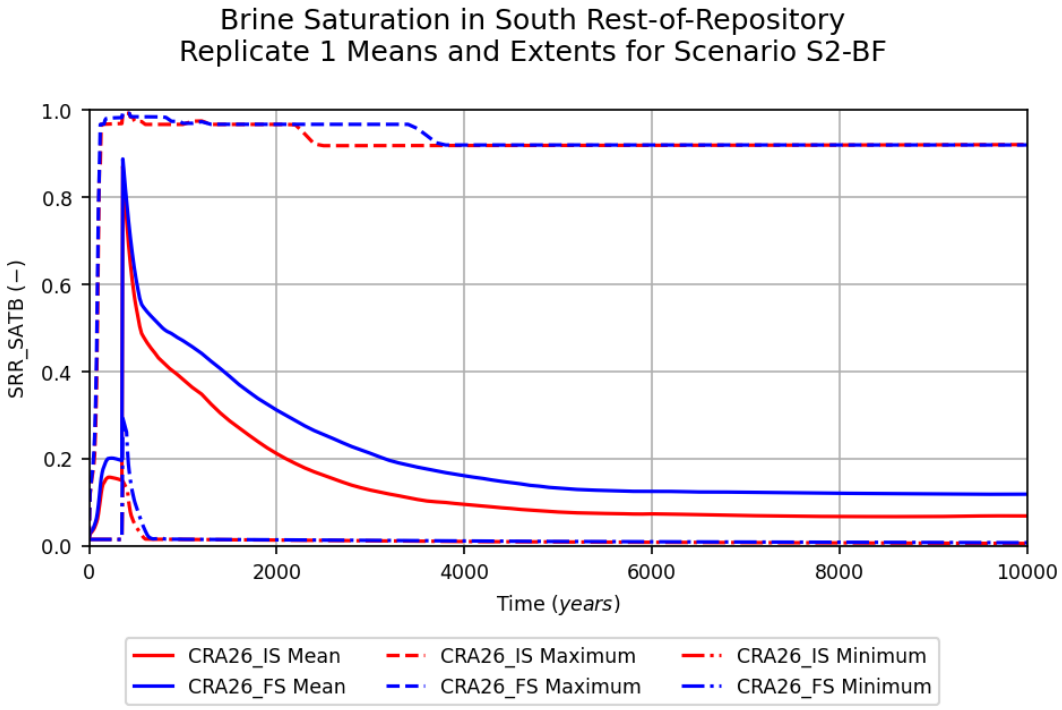


Figure PA-A-18. Minimum, Maximum, and Mean of SROR Brine Saturation, Scenario S2-BF

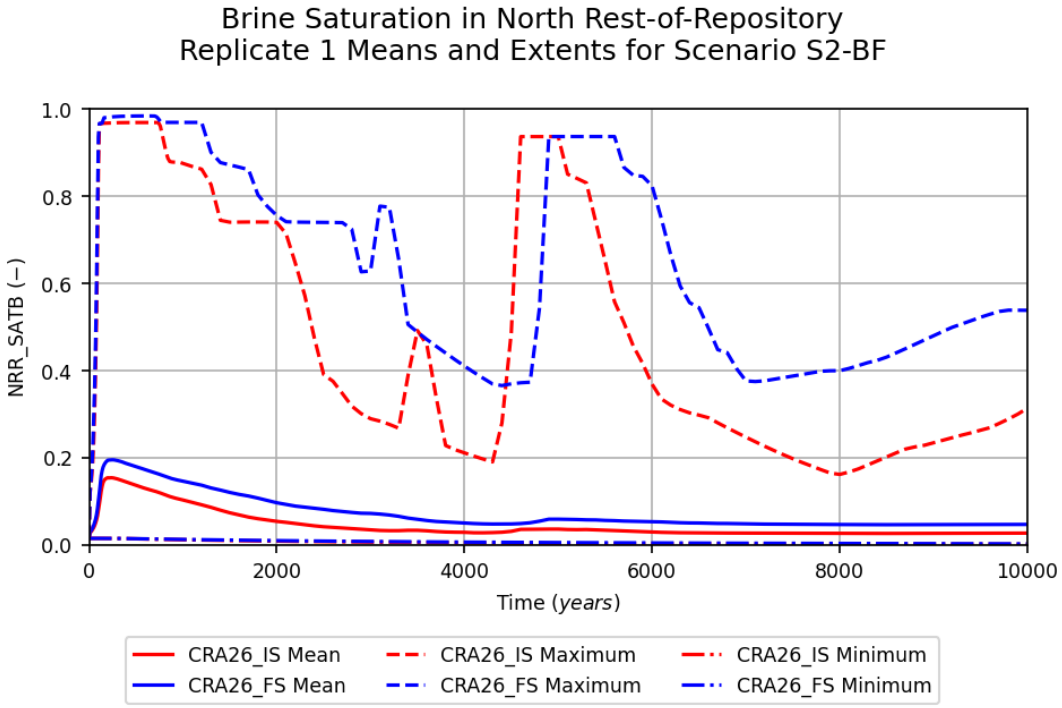


Figure PA-A-19. Minimum, Maximum, and Mean of NROR Brine Saturation, Scenario S2-BF

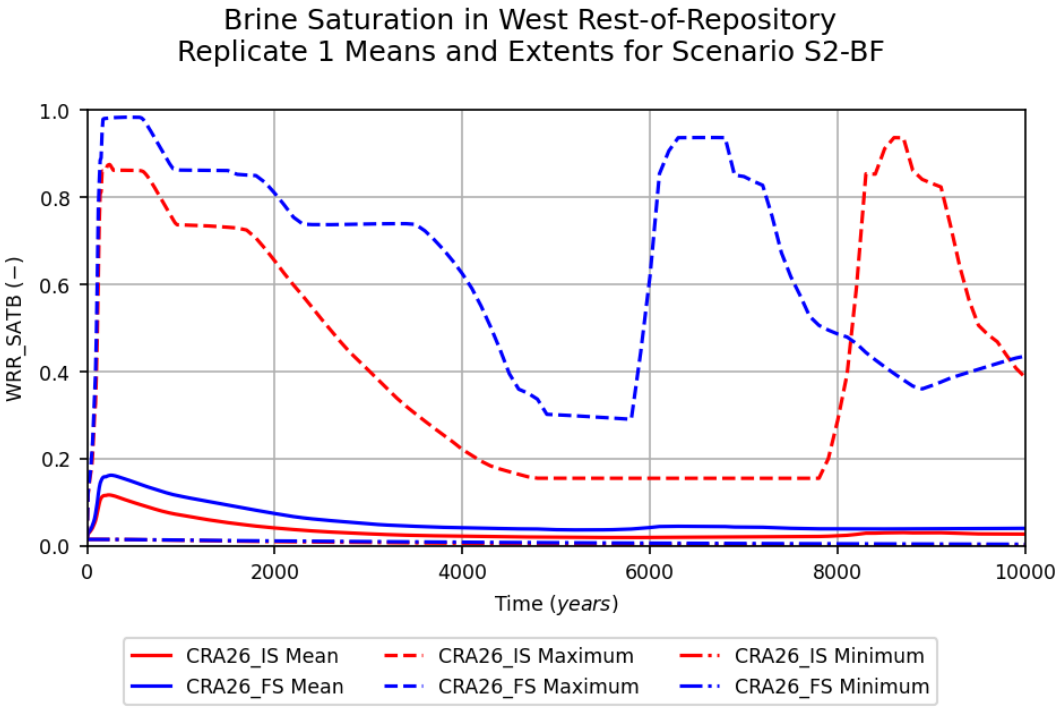


Figure PA-A-20. Minimum, Maximum, and Mean of WROR Brine Saturation, Scenario S2-BF

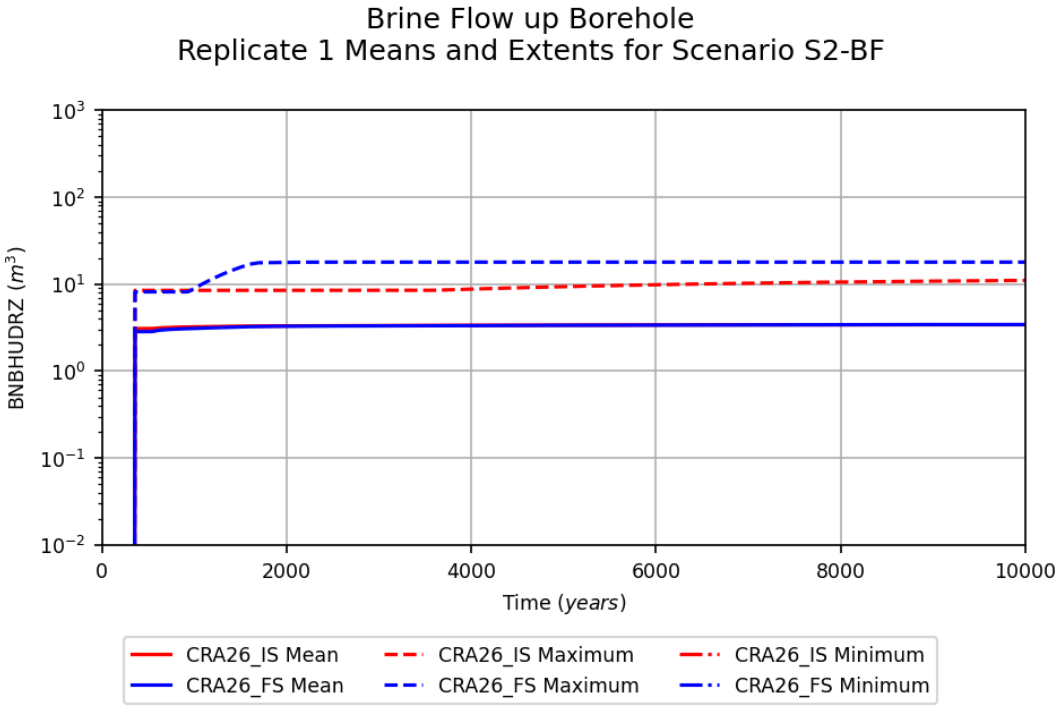


Figure PA-A-21. Minimum, Maximum, and Mean Cumulative Brine Flow up the Borehole, Scenario S2-BF.

PA-A-5.1.2 Fluid Flow in the Salado for E2 Intrusion Scenarios

E2 intrusion scenarios represent drilling events that intersect a waste-filled panel but do not encounter a pressurized brine reservoir beneath the repository. Figure PA-A-22 through Figure PA-A-25 show the minimum, maximum, and mean pressures in the WP, SROR, NROR, and WROR regions for the CRA26_FS and compare to the CRA26_IS. The results indicate that pressures for S4-BF scenario (Appendix PA, Section PA-6.3.1) are increased in the CRA26_FS repository compared to the CRA26_IS repository. Zeitler et al. (2025) attribute this increase to the larger repository footprint and reduced brine consumption, which result in higher brine availability and increased brine saturation in some waste areas.

Figures PA-A-26 through PA-A-29 show the minimum, maximum, and mean brine saturations in the WP, SROR, NROR, and WROR regions for the CRA26_FS and compare to the CRA26_IS. Results for S4-BF scenarios indicate that brine saturations are generally increase in the CRA26_FS repository compared to the CRA26_IS repository. This increase is consistent with the reduced brine consumption observed in undisturbed scenarios and S2-BF scenarios, which leads to higher brine saturation levels in waste areas under S4-BF conditions.

Cumulative brine flows up the intrusion borehole potentially transports contaminants to the ground surface or to the Culebra, where contaminants may transport laterally through the Culebra to the LWB. Maximum and mean brine flows up the intrusion borehole for S4-BF scenarios are plotted in Figure PA-A-30. Brine flow up the borehole for CRA26_FS is increased compared to CRA26_IS but remains small in S4-BF scenarios relative to S2-BF scenarios (Figure PA-A-21).

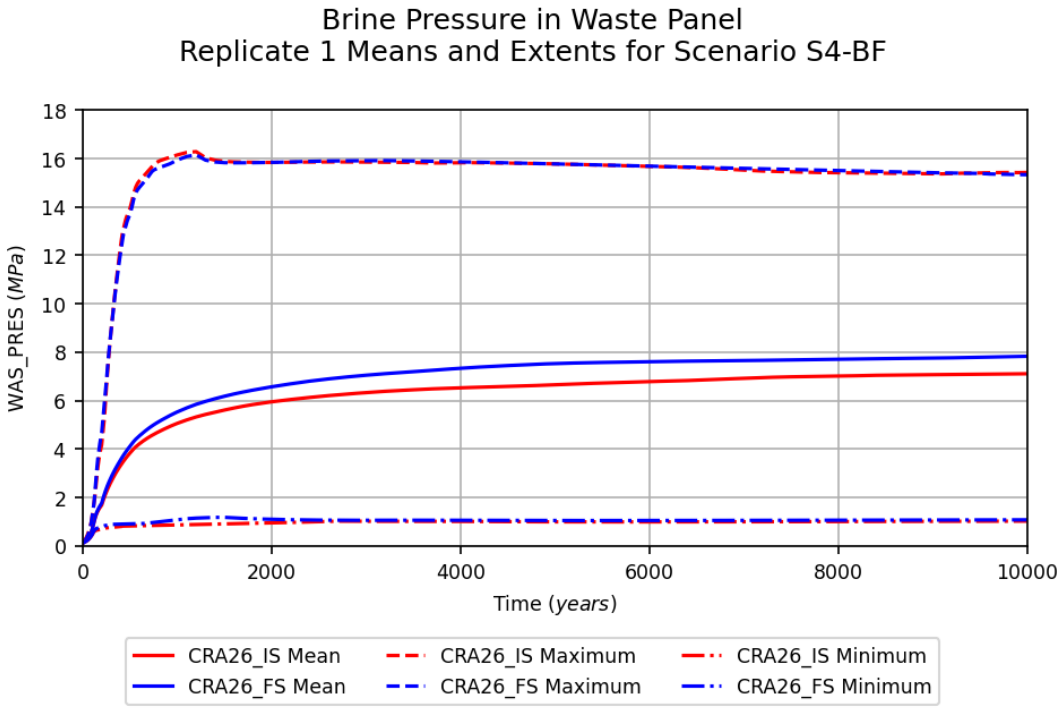


Figure PA-A-22. Minimum, Maximum, and Mean of WP Pressure, Scenario S4-BF

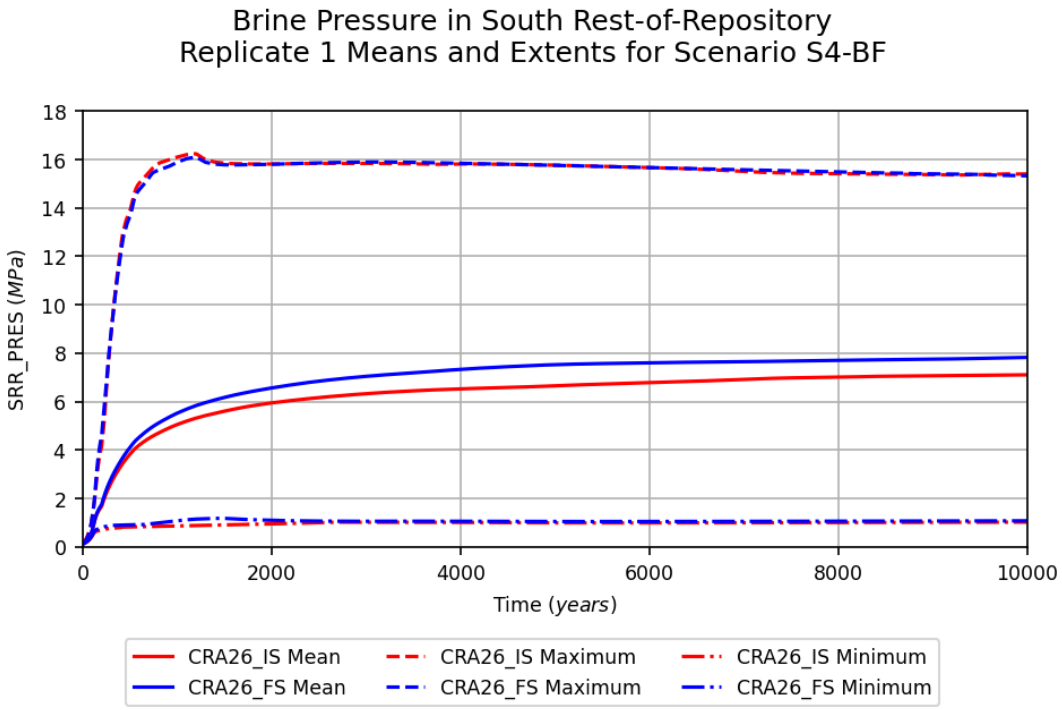


Figure PA-A-23. Minimum, Maximum, and Mean of SROR Pressure, Scenario S4-BF

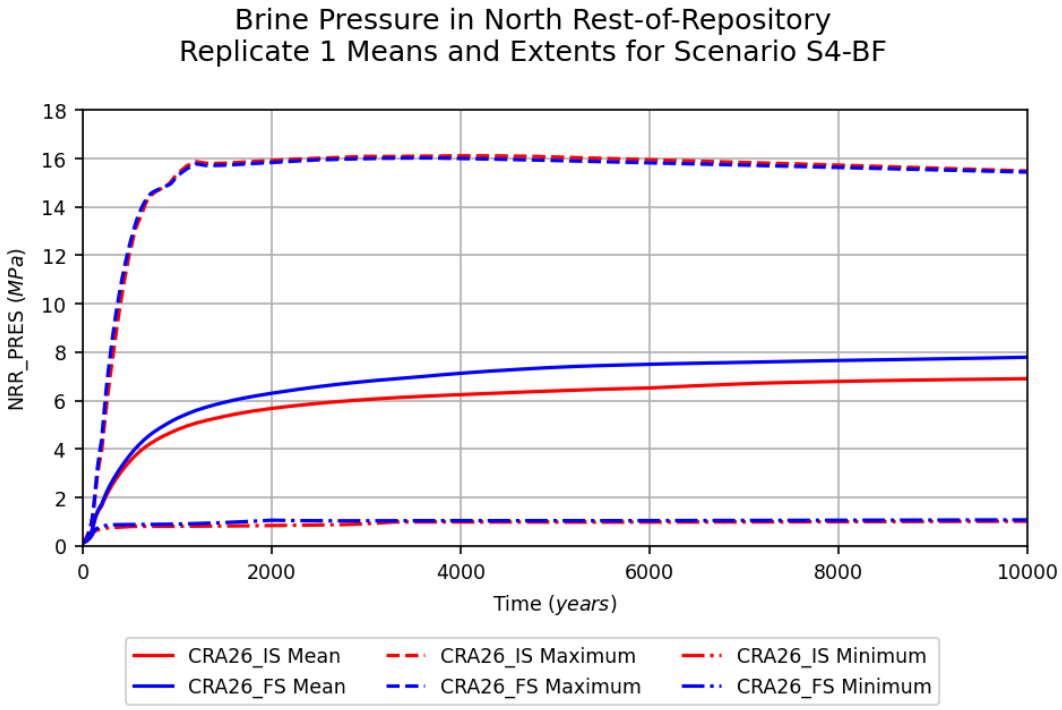


Figure PA-A-24. Minimum, Maximum, and Mean of NROR Pressure, Scenario S4-BF

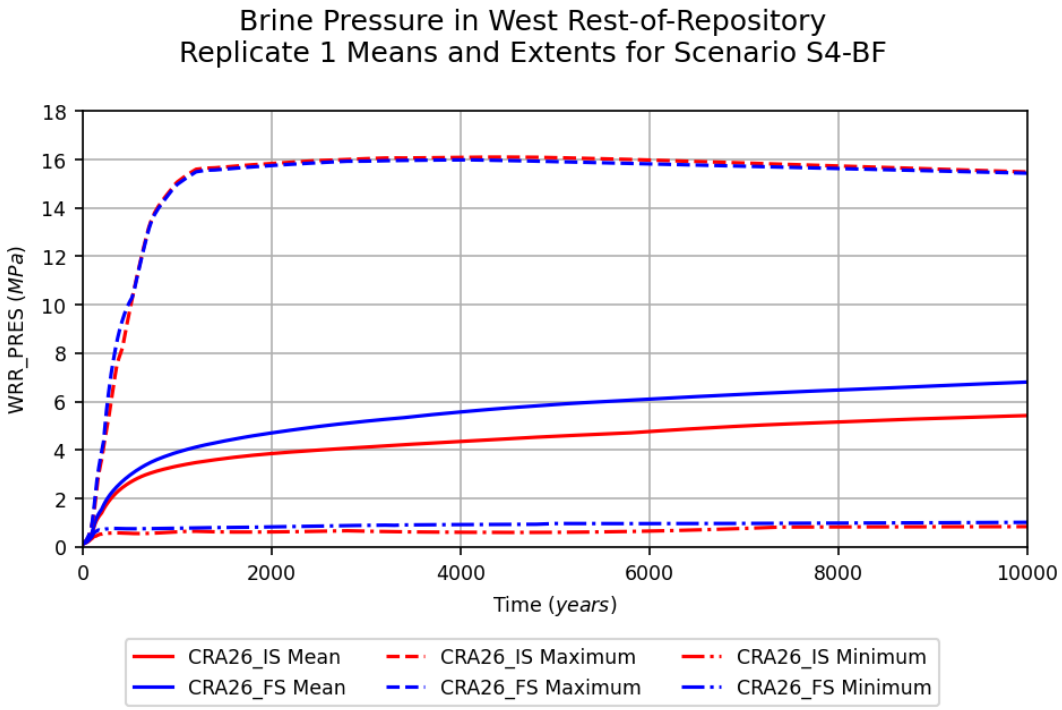


Figure PA-A-25. Minimum, Maximum, and Mean of WROR Pressure, Scenario S4-BF

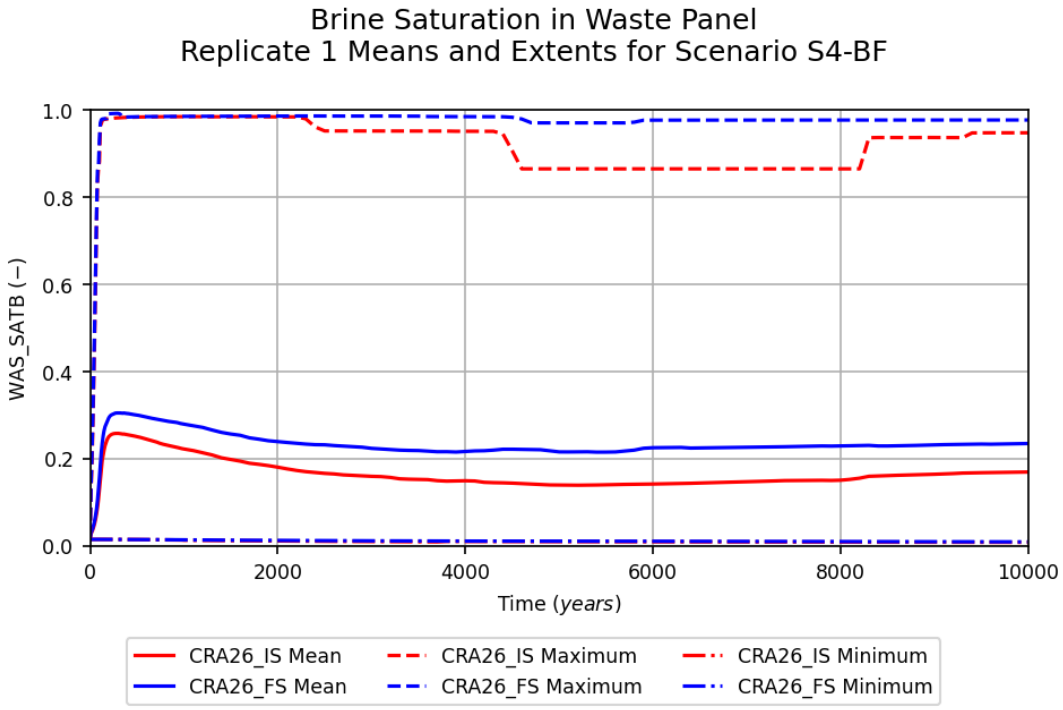


Figure PA-A-26. Minimum, Maximum, and Mean of WP Brine Saturation, Scenario S4-BF

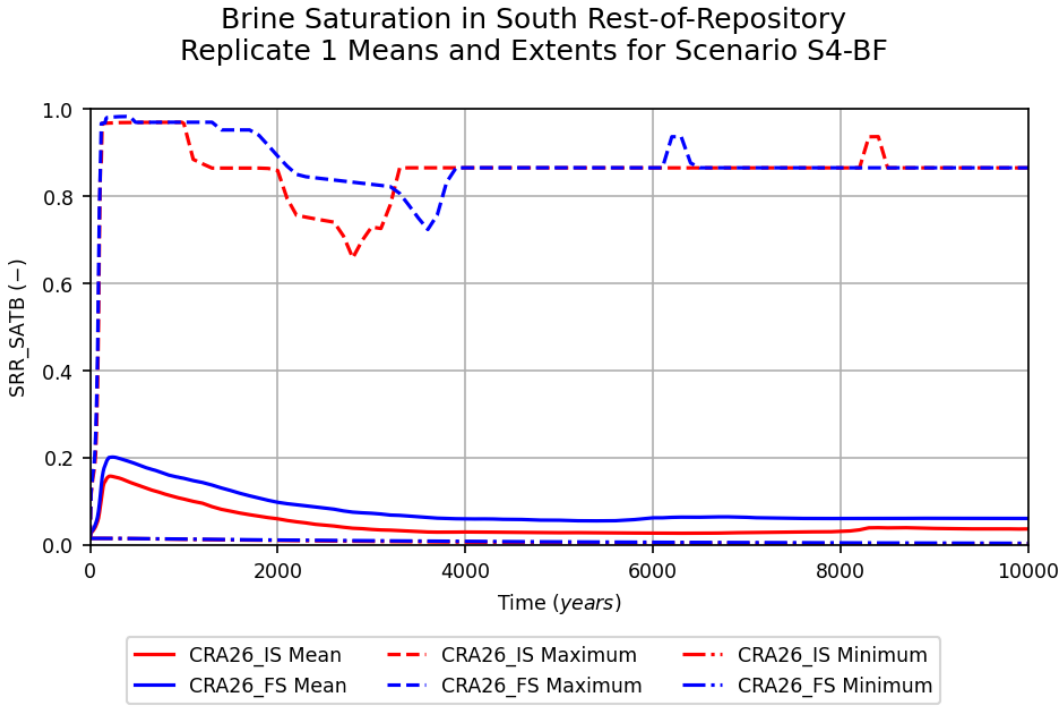


Figure PA-A-27. Minimum, Maximum, and Mean of SROR Brine Saturation, Scenario S4-BF

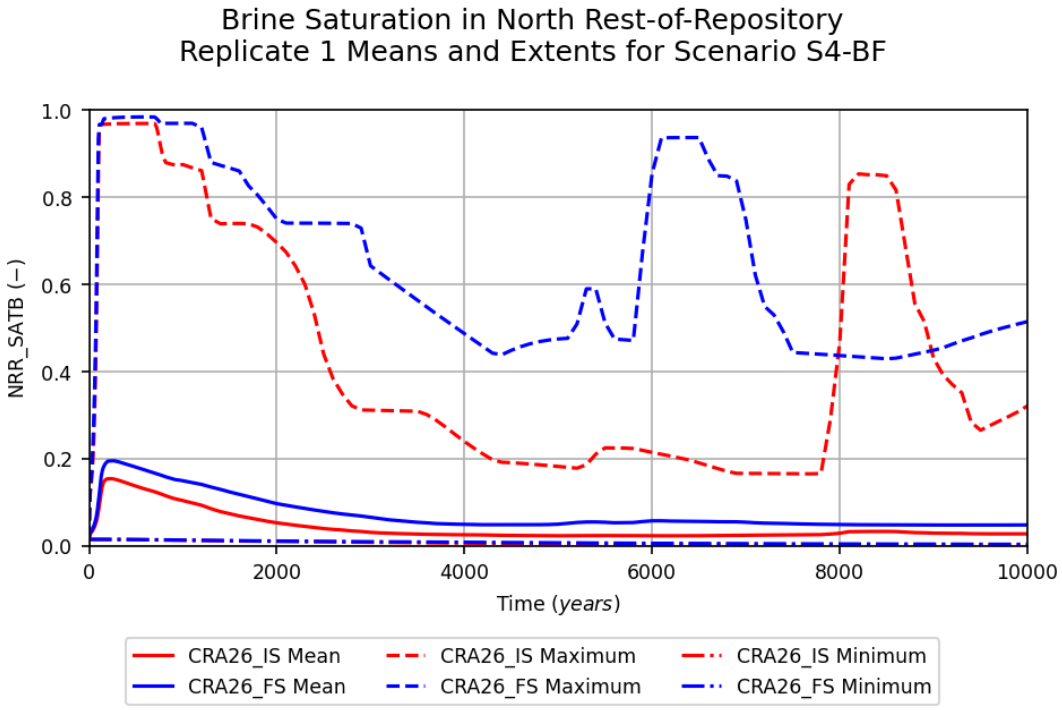


Figure PA-A-28. Minimum, Maximum, and Mean of NROR Brine Saturation, Scenario S4-BF

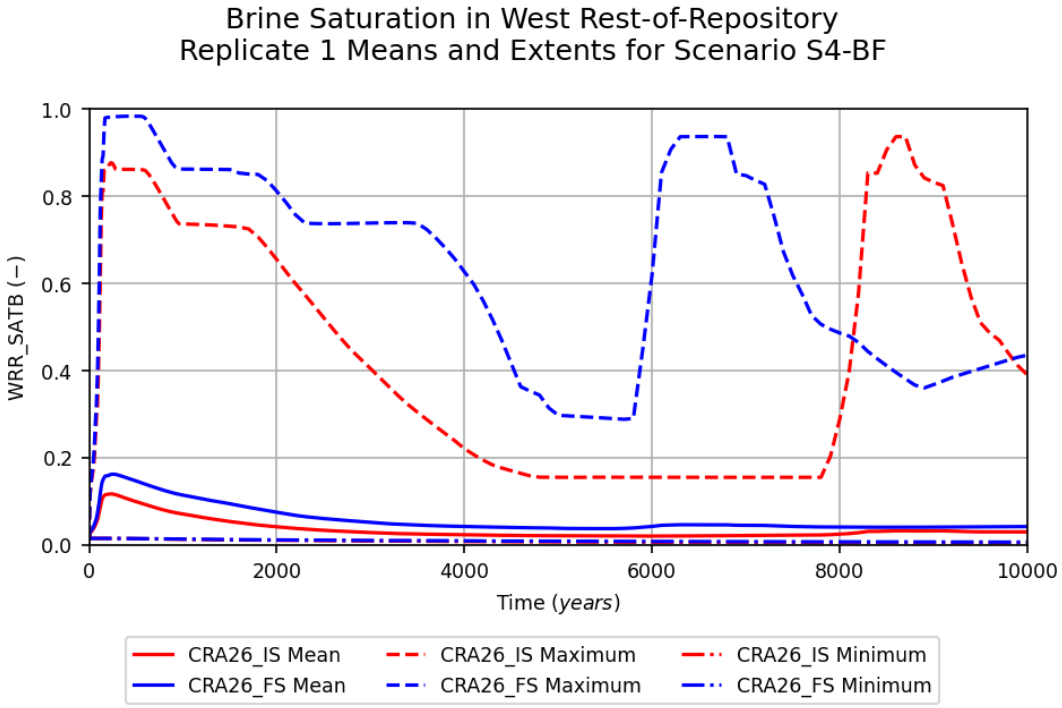


Figure PA-A-29. Minimum, Maximum, and Mean of WROR Brine Saturation, Scenario S4-BF

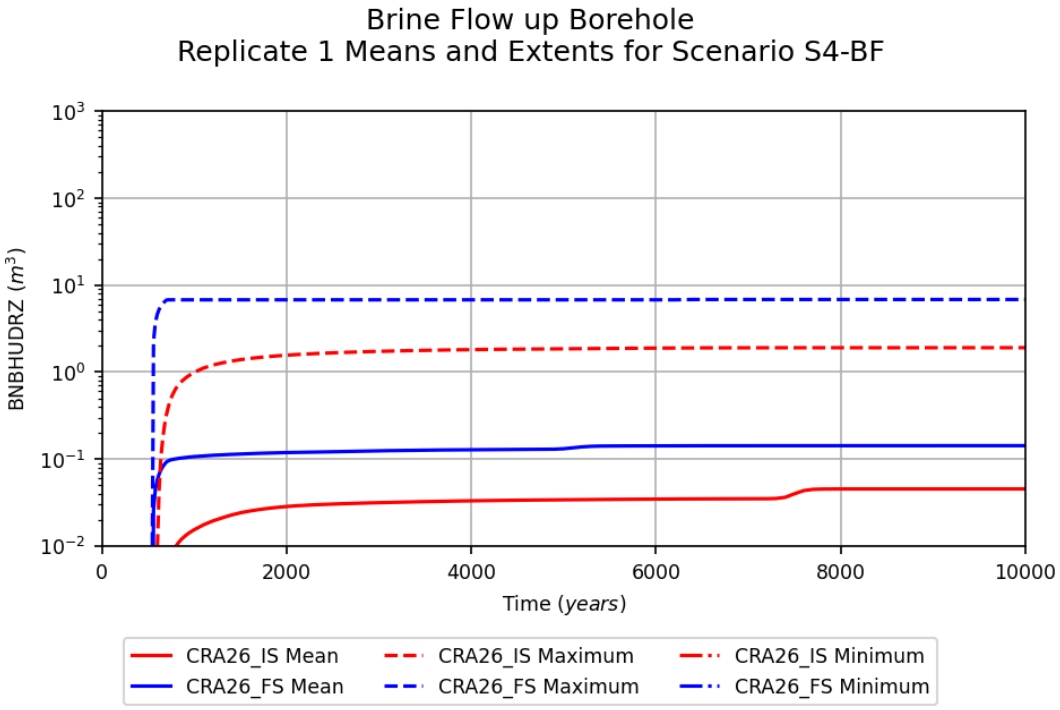


Figure PA-A-30. Minimum, Maximum, and Mean Cumulative Brine Flow up the Borehole, Scenario S4-BF.

PA-A-5.1.3 Summary of Fluid Flow in the Salado

This section provides summarized results of all Salado flow modeling, including scenarios S1-BF, S2-BF, S4-BF, and S6-BF (Appendix PA, Section PA-6.3.1). Table PA-A-3 contains summary statistics for pressures, Table PA-A-4 contains summary statistics for brine saturations, and Table PA-A-5 contains summary statistics for brine flows. These tables present means and maxima over the 10,000-year regulatory period. Brine flow statistics include flows into the repository, up the shaft, and up the intrusion borehole.

Table PA-A-3. Pressure (MPa) Statistics on Replicate 1 Means

Quantity	Scenario	CRA26_IS Mean Value[1]	CRA26_FS Mean Value[1]	CRA26_IS Max Value[2]	CRA26_FS Max Value[2]
Waste Panel Pressure	S1-BF	6.7	7.3	7.7	8.5
Waste Panel Pressure	S2-BF	11.5	11.3	12.7	12.6
Waste Panel Pressure	S4-BF	6.3	7.0	7.1	7.8
Waste Panel Pressure	S6-BF	8.8	8.9	10.3	10.3
SROR Pressure	S1-BF	6.7	7.3	7.7	8.5
SROR Pressure	S2-BF	11.5	11.3	12.7	12.5
SROR Pressure	S4-BF	6.3	7.0	7.1	7.8
SROR Pressure	S6-BF	8.8	8.9	10.3	10.3
NROR Pressure	S1-BF	6.3	7.0	7.3	8.2
NROR Pressure	S2-BF	10.1	9.9	11.0	10.9
NROR Pressure	S4-BF	6.0	6.8	6.9	7.8
NROR Pressure	S6-BF	8.1	8.3	9.4	9.5
South Ops Pressure	S1-BF	3.2	4.3	4.9	6.2
South Ops Pressure	S2-BF	5.4	5.6	7.9	8.0
South Ops Pressure	S4-BF	3.1	4.2	4.7	6.0
South Ops Pressure	S6-BF	4.3	4.9	6.7	7.2
Exp Area Pressure	S1-BF	3.2	4.2	4.9	6.1
Exp Area Pressure	S2-BF	5.4	5.6	7.8	8.0
Exp Area Pressure	S4-BF	3.1	4.2	4.6	6.0
Exp Area Pressure	S6-BF	4.3	4.9	6.7	7.2
West Ops Pressure	S1-BF	3.2	4.2	4.9	6.1
West Ops Pressure	S2-BF	5.4	5.6	7.8	7.9
West Ops Pressure	S4-BF	3.1	4.2	4.6	6.0
West Ops Pressure	S6-BF	4.3	4.9	6.7	7.2
WROR Pressure	S1-BF	4.5	5.5	5.6	6.9
WROR Pressure	S2-BF	6.4	6.7	8.4	8.5
WROR Pressure	S4-BF	4.4	5.5	5.4	6.8
WROR Pressure	S6-BF	5.5	6.1	7.4	7.9

Notes:

1 Average over the time interval (0-10,000 years) of the Replicate 1 mean.

2 Maximum over the time interval (0-10,000 years) for the Replicate 1 mean.

Table PA-A-4. Brine Saturation Statistics on Replicate 1 Means

Quantity	Scenario	CRA26_IS Mean Value[1]	CRA26_FS Mean Value[1]	CRA26_IS Max Value[2]	CRA26_FS Max Value[2]
Waste Panel Saturation	S1-BF	0.14	0.20	0.26	0.31
Waste Panel Saturation	S2-BF	0.34	0.45	0.92	0.93
Waste Panel Saturation	S4-BF	0.16	0.23	0.26	0.31
Waste Panel Saturation	S6-BF	0.27	0.35	0.54	0.58
SROR Saturation	S1-BF	0.04	0.06	0.16	0.20
SROR Saturation	S2-BF	0.14	0.20	0.87	0.89
SROR Saturation	S4-BF	0.05	0.08	0.16	0.20
SROR Saturation	S6-BF	0.07	0.10	0.26	0.28
NROR Saturation	S1-BF	0.04	0.07	0.15	0.20
NROR Saturation	S2-BF	0.04	0.07	0.15	0.20
NROR Saturation	S4-BF	0.04	0.07	0.15	0.20
NROR Saturation	S6-BF	0.04	0.07	0.15	0.20
South Ops Saturation	S1-BF	0.53	0.59	0.58	0.65
South Ops Saturation	S2-BF	0.50	0.57	0.54	0.62
South Ops Saturation	S4-BF	0.53	0.59	0.58	0.65
South Ops Saturation	S6-BF	0.52	0.58	0.56	0.63
Exp Area Saturation	S1-BF	0.15	0.22	0.16	0.25
Exp Area Saturation	S2-BF	0.14	0.22	0.16	0.24
Exp Area Saturation	S4-BF	0.15	0.22	0.16	0.25
Exp Area Saturation	S6-BF	0.14	0.22	0.16	0.24
West Ops Saturation	S1-BF	0.01	0.02	0.09	0.09
West Ops Saturation	S2-BF	0.01	0.02	0.09	0.09
West Ops Saturation	S4-BF	0.01	0.02	0.09	0.09
West Ops Saturation	S6-BF	0.01	0.02	0.09	0.09
WROR Saturation	S1-BF	0.03	0.06	0.12	0.16
WROR Saturation	S2-BF	0.03	0.06	0.12	0.16
WROR Saturation	S4-BF	0.03	0.06	0.12	0.16
WROR Saturation	S6-BF	0.03	0.06	0.12	0.16

Notes:

1 Average over the time interval (0-10,000 years) of the Replicate 1 mean.

2 Maximum over the time interval (0-10,000 years) for the Replicate 1 mean.

Table PA-A-5. Brine Flow (m^3) Statistics for Replicate 1

Quantity	Scenario	CRA26_IS Mean Value[1]	CRA26_FS Mean Value[1]	CRA26_IS Max Value[2]	CRA26_FS Max Value[2]
Brine Flow into Repository	S1-BF	4.20E+04	6.37E+04	2.44E+05	3.42E+05
Brine Flow into Repository	S2-BF	6.62E+04	8.38E+04	2.51E+05	3.38E+05
Brine Flow into Repository	S4-BF	4.21E+04	6.37E+04	2.55E+05	3.59E+05
Brine Flow into Repository	S6-BF	4.96E+04	6.89E+04	2.38E+05	3.42E+05
Brine Flow up Shaft [3]	S1-BF	2.71E+00	3.79E+00	3.43E+01	3.67E+01
Brine Flow up Shaft [3]	S2-BF	5.13E+00	5.39E+00	2.96E+01	3.55E+01
Brine Flow up Shaft [3]	S4-BF	2.41E+00	3.73E+00	2.93E+01	3.54E+01
Brine Flow up Shaft [3]	S6-BF	3.89E+00	4.58E+00	2.93E+01	3.26E+01
Brine Flow up Borehole [4]	S1-BF[5]	-	-	-	-
Brine Flow up Borehole [4]	S2-BF	3.41E+00	3.43E+00	1.10E+01	1.79E+01
Brine Flow up Borehole [4]	S4-BF	4.53E-02	1.42E-01	1.91E+00	6.84E+00
Brine Flow up Borehole [4]	S6-BF	5.94E-01	9.46E-01	1.04E+01	2.38E+01

Notes:
1 Replicate 1 mean at 10,000 years.
2 Maximum over all 100 Replicate 1 vectors at 10,000 years.
3 As measured at the shaft intersection with Marker Bed 138.
4 As measured at the borehole intersection with Marker Bed 138.
5 "-" indicates "not applicable," as there is no borehole in the S1-BF scenario

PA-A-5.1.4 Fluid Flow in the Culebra

Figure PA-A-31 shows the ensemble average of $\log_{10}$ flow rates within the LWB for no mining, as well as full and partial mining for the CRA26_FS. Flow fields from simulations without mining (no mining) are not directly considered in PA calculations but serve as input to the mining modified (full and partial) flow fields. Flow field results are identical to the CRA26_IS.

The most prominent feature in the no-mining flow rate results is a pseudo-linear north-south high-transmissivity pathway located in the southern half of the domain. Without mining, flow is generally oriented toward the south (Wilgus and Bethune 2025, Section 8.2).

Full and partial mining scenario modifications create sharp flow rate gradients at the edges of the impacted areas. The edges lead to more variation in the mining modified flow fields producing a quasi-rectangular shape just inside the LWB in the partial mining case, and an irregular shaped region in the full mining case. Flow in the mining modified cases is generally directed toward the south similar to no mining flow results. However, particles entering the Culebra over the westernmost panels (Figure PA-A-3; CRP 4, Panels 15, 16, 17, and 18) in the

full mining case generally follow a distinct southward path along the western edge of the mining-impacted area (see section 5.2 in Wilgus and Bethune 2025).

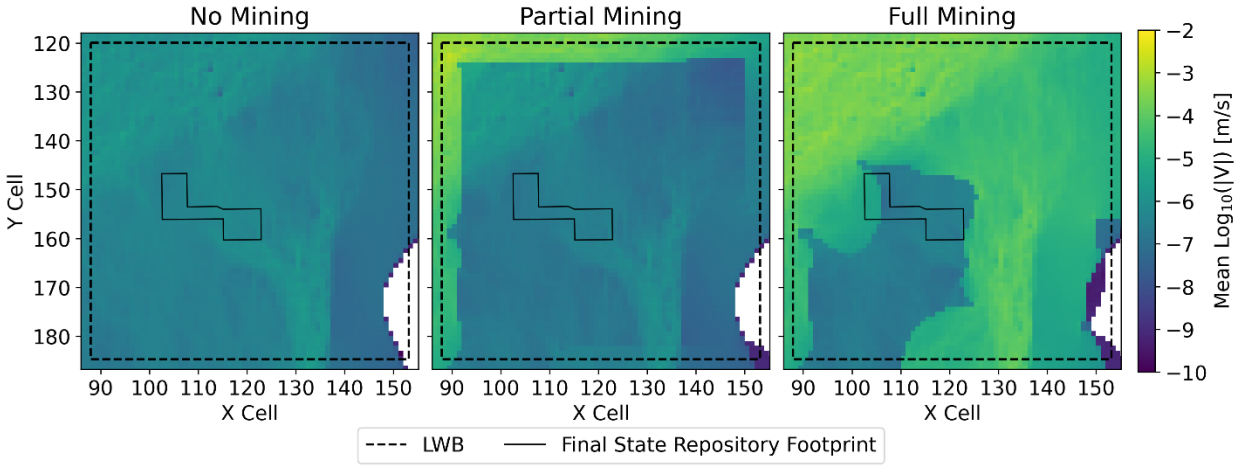


Figure PA-A-31. Ensemble Mean Flow Rates

PA-A-5.2 Radionuclide Transport

This section summarizes the CRA26_FS radionuclide transport results for the disturbed repository scenarios highlighting differences from the CRA26_IS results. Radionuclide transport in the Salado is calculated by the code NUTS (see Appendix PA Section PA-6.3.2). Radionuclide transport from the Salado to the Culebra is calculated by NUTS and PANEL (see Appendix PA Sections PA-6.3.2 and PA-6.3.5.3). Radionuclide transport within the Culebra is calculated by SECOTP2D (see Appendix PA Section PA-6.3.10). For all radionuclide transport calculations, mobilized concentrations of radionuclides in Salado and Castile brines are computed by the code PANEL (see Appendix PA Section PA-6.3.5.1).

Radionuclide transport results for the CRA26_FS are presented in Zeitler et al. (2025). The CRA26_FS introduces radionuclide transport pathways in the Culebra unique to the westernmost panels (Panels 14 through 19), which are represented by CRP 3 and CRP 4 in the transport modeling.

PA-A-5.2.1 Mobilized Radionuclide Concentrations

Calculation of mobilized radionuclide concentrations accounts for radionuclide decay and ingrowth, which influence the inventory and mobilized concentrations of radionuclides in brine. The mean mobile concentrations for lumped radionuclides in 1× the minimum Castile brine volume (see Appendix PA, Section PA-4.3.2) are shown in Figure PA-A-32. Results for Salado brine exhibit the same qualitative temporal behavior and dominant radionuclides as those shown for Castile brine.

The U.S. Environmental Protection Agency (EPA) defines a normalized activity measure called EPA Units. Radionuclide concentrations are expressed in EPA units/m³ to combine the

radioactivity of different isotopes. The mean total radioactivity concentration at early times is dominated by ^{241}Am, while at later times it is dominated by ^{239}Pu. The mean total radioactivity concentration (denoted as CDBR in Figure PA-A-32) for CRA26_FS is slightly below the CRA26_IS concentration for most of the 10,000-year regulatory period. However, at late times, the CRA26_FS concentration becomes very slightly higher than the CRA26_IS concentration.

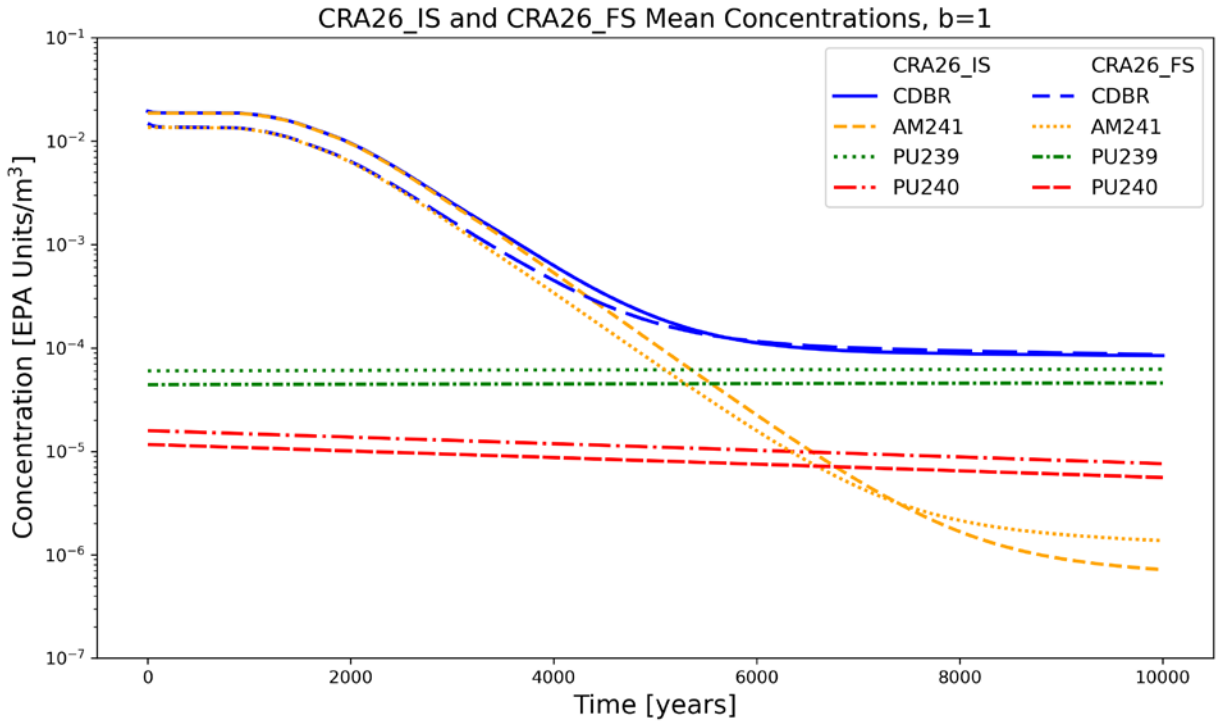


Figure PA-A-32. Mean Mobilized Radionuclide Concentrations Vs Time. Castile (ERDA-6) Brine

PA-A-5.2.2 Transport through MBs and Shaft

In the disturbed repository scenarios, none of the 300 realizations of the CRA26_FS resulted in releases through the marker beds that exceed the screening limit. No realization showed transport of radionuclides through the shaft to the Culebra in the CRA26_FS.

PA-A-5.2.3 Transport to the Culebra

Radionuclide transport to the Culebra via a single intrusion borehole (disturbed scenarios S2-BF, S3-BF, S4-BF, and S5-BF) is modeled using the code NUTS (see Appendix PA Section PA-6.3.2). Transport to the Culebra in the multiple intrusion scenario (S6-BF) is modeled using the code PANEL (see Appendix PA Section PA-6.3.3.3). For all scenarios, radionuclide discharge through the borehole is influenced by brine discharge volumes and radionuclide concentration limits, which are calculated using PANEL (see Appendix PA Section PA-6.3.3.1).

Figure PA-A-33 and Figure PA-A-34 illustrate the cumulative brine discharge and cumulative lumped radionuclide release through the intrusion borehole for disturbed repository scenarios S2-BF through S5-BF. Results for CRA26_FS show mixed trends in radionuclide discharge, reflecting the interplay between brine discharge volumes and radionuclide solubilities. High radionuclide solubilities are not necessarily correlated with high brine discharge volumes, leading to variability in radionuclide releases across vectors. For scenarios S4-BF and S5-BF, the CRA26_IS radionuclide discharges are all below the cutoff of the plot, while a few vectors in the CRA26_FS have discharges that are visible.

Mean brine discharges are slightly increased in all intrusion scenarios in CRA26_FS compared to CRA26_IS. This increase is attributed to higher brine pressures and saturations in the FS repository, which result from the expanded repository footprint and reduced brine consumption. Mean radionuclide discharges are increased in single intrusion scenarios (S2-BF, S3-BF, S4-BF, and S5-BF). For scenarios S4-BF and S5-BF, no vectors are screened in for the CRA26_IS, whereas a small number of vectors are screened in for the CRA26_FS (two vectors for S4-BF and one vector for S5-BF). These screened-in realizations result in nonzero radionuclide discharges for the CRA26_FS, whereas all CRA26_IS releases for these scenarios remain below the screening threshold and are therefore not plotted (Zeitler et al. 2025, Section 4.6). For the multi-intrusion scenario (S6-BF), mean and maximum radionuclide discharges are similar to the CRA26_IS results, though the median discharge increases.

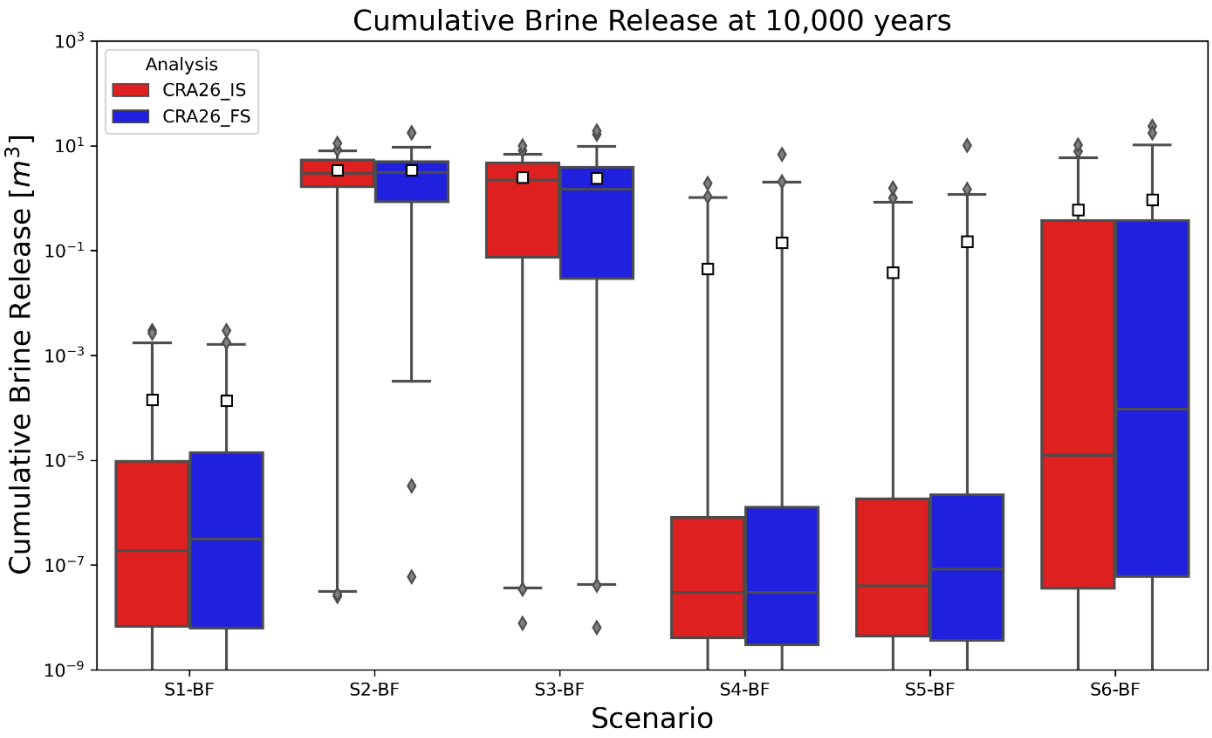


Figure PA-A-33. Cumulative Brine Releases up the Borehole[1]

[1] Boxplots are used to facilitate visualizing and comparing distributions of results. The convention used in this section is that the "box" bottom and top edges indicate the 25th and 75th percentiles, the box interior line indicates the 50th percentile (median), and the square marker indicates the mean. The "whiskers" (the extended vertical lines with horizontal bars) indicate the 2nd and 98th percentiles, and the diamond markers exterior to the bars are discrete outliers (i.e., less than the 2nd percentile or greater than the 98th percentile).

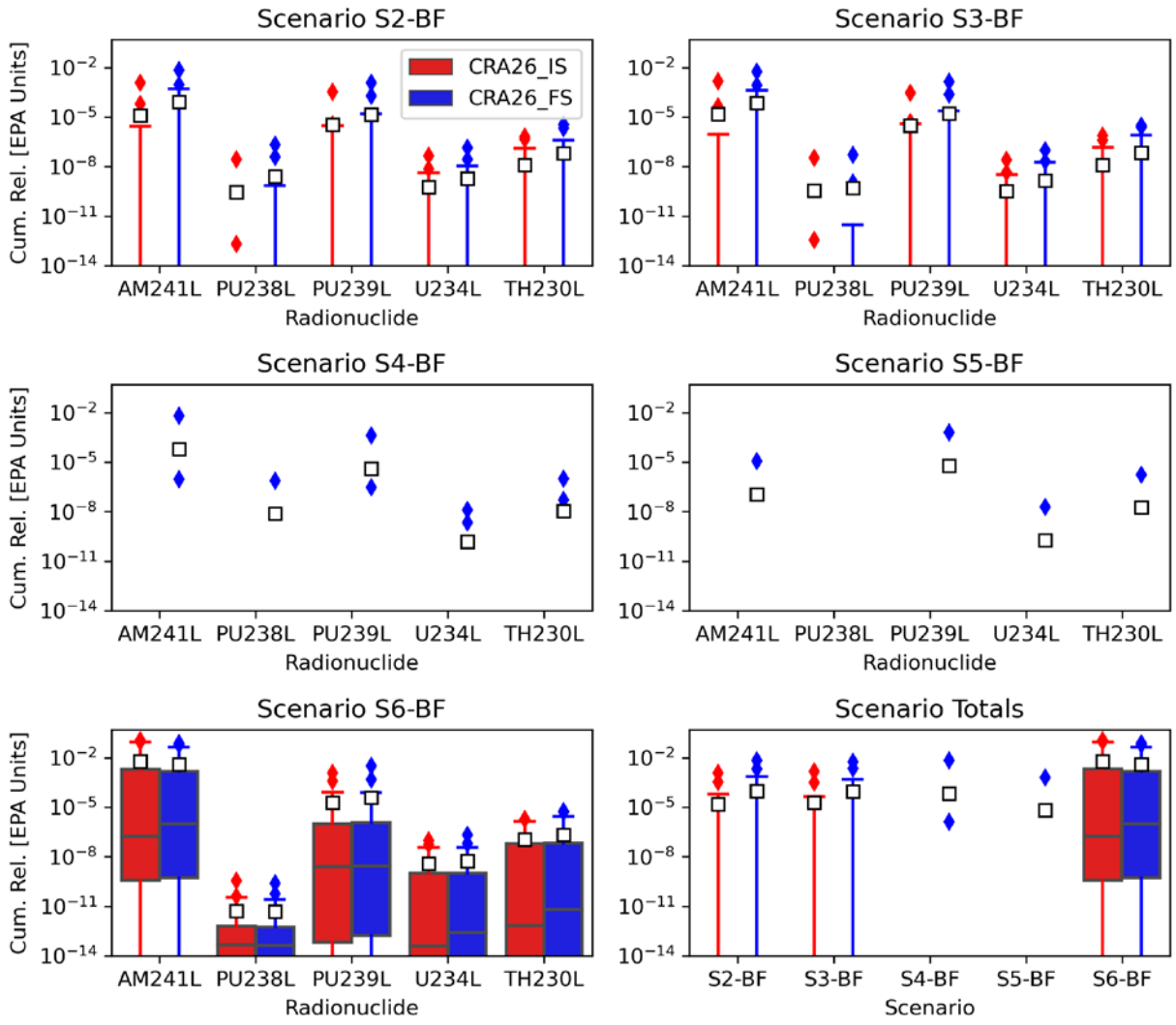


Figure PA-A-34. Cumulative Lumped Radionuclide Release[1]

PA-A-5.2.4 Transport through the Culebra

The CRA26_FS considers four CRPs (CRP 1, CRP 2, CRP 3, and CRP 4) while the CRA26_IS only considers CRP 1 and CRP 2. Consequently, CRP 1 and CRP 2 results are identical between the CRA26_FS and CRA26_IS.

Figure PA-A-35 and Figure PA-A-36 show CRA26_FS exceedance probability curves of cumulative mass of each tracked radionuclide reaching the LWB by 10,000 years for full and partial mining scenarios, respectively. Mass discharge is shown on a logarithmic scale on the x-axis from 10^{-9} to 1 kg. Some partial mining scenario subplots display no results due to the low predictions of mass to the LWB. A full set of replicate statistics are provided in Wilgus and Bethune (2025).

Cumulative releases at 10,000 years are higher in the full mining scenario than in the partial mining scenario for all radionuclides across all displayed probability ranges. The differences are most apparent in CRP 4 where full mining scenario results are significantly larger than partial mining results. In the full mining scenario, CRP 2 and CRP 3 releases are generally lower than CRP 1, which in turn are lower than CRP 4, for all radionuclides. Particles from CRP 4 travel a different southward path than other CRPs (see section 5.2 in Wilgus and Bethune 2025) leading to shorter travel times and larger cumulative discharge of mass (Section PA-A-6.4). Amongst the radionuclides, ^{241}Am shows the lowest releases, while ^{234}U, shows the highest releases in both the full and partial mining scenarios.

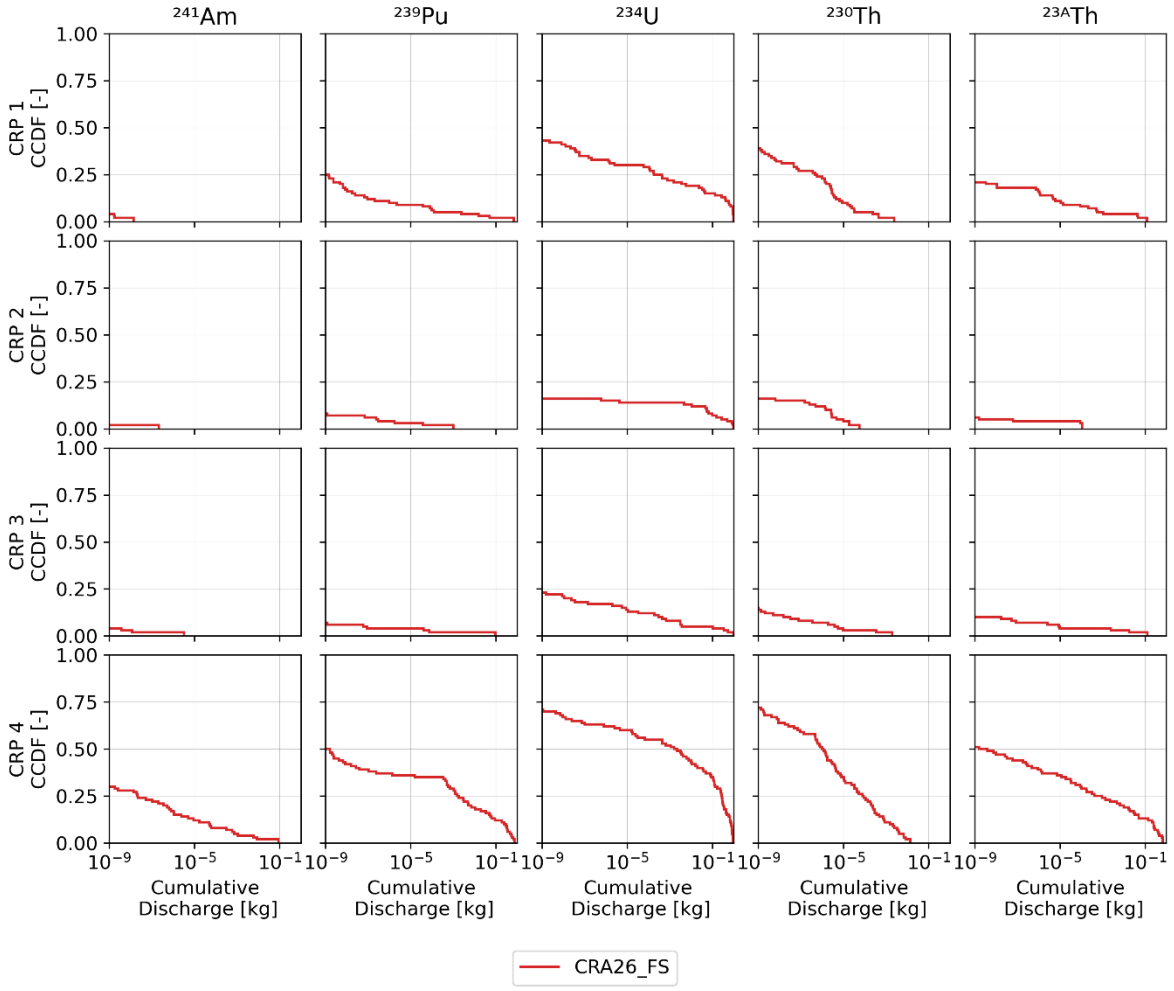


Figure PA-A-35. Exceedance Probability of Cumulative Mass to the LWB in 10,000 Years for Full Mining Scenario.

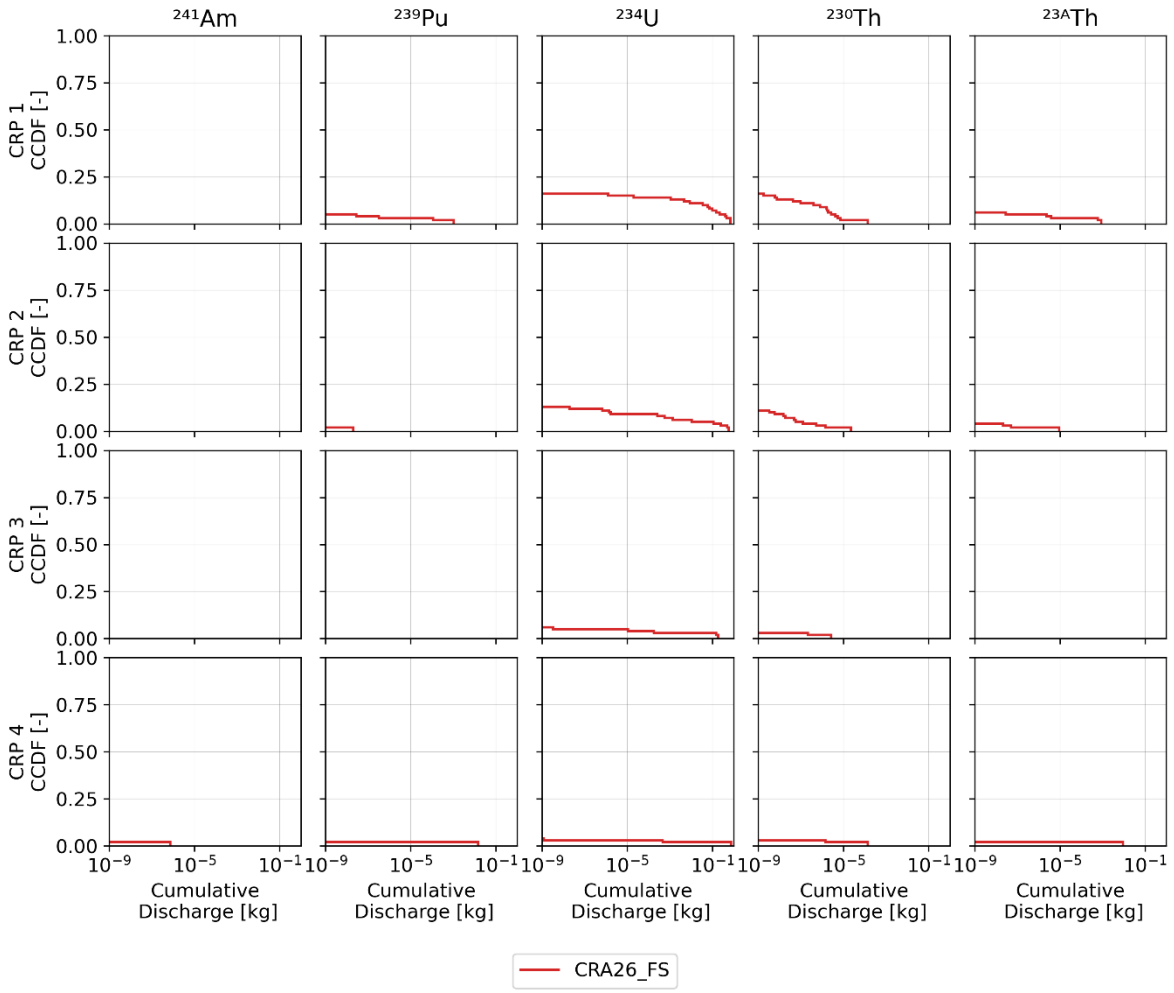


Figure PA-A-36. Exceedance Probability of Cumulative Mass to the LWB in 10,000 Years for Partial Mining Scenario.

PA-A-5.3 Direct Releases

Direct releases occur at the time of a drilling intrusion and include cuttings and cavings, spallings, and DBRs. This section presents an analysis of the volume released by each mechanism, while Section 6.0 presents the normalized radionuclide releases by each mechanism.

The results presented in this section highlight the impact of the increased repository footprint and waste inventory, as well as the modifications to repository parameters and radionuclide concentrations associated with the FS configuration, on direct release mechanisms. This includes comparisons with the IS repository results documented in Appendix PA. Additional descriptions of the cuttings, cavings, spallings, and DBRs calculated for the CRA26_FS PA are provided by Zeitler et al. (2025).

PA-A-5.3.1 Cuttings and Cavings

Cuttings and cavings releases occur during drilling intrusions when waste material is removed by the drill bit or eroded into the borehole fluid.

Cavings area results, calculated by the WIPP PA code CUTTINGS_S, are identical between the CRA26_FS and CRA26_IS analyses because the input parameters and methodology used to calculate cavings remain unchanged. Cavings area replicate statistics for the CRA26_FS are summarized in Table PA-A-6, including the mean cavings area, mean nonzero cavings area, maximum cavings area, and the number of realizations without cavings. These statistics are the same for both analyses, reflecting the unchanged cavings model inputs.

Table PA-A-6. Caving Area Statistics for CRA26_FS and CRA26_IS

Replicate	Mean Cavings Area (m^2)	Mean Non-Zero Cavings Area (m^2)	Maximum Cavings Area (m^2)	Number of Vectors without Cavings
1	0.011	0.021	0.110	49
2	0.010	0.019	0.107	44
3	0.011	0.021	0.090	49

PA-A-5.3.2 Spallings

Spallings releases occur when repository pressures exceed the hydrostatic pressure of the drilling fluid column during a drilling intrusion, resulting in the expulsion of waste material from the repository into the borehole. Spallings releases are influenced primarily by repository pressure and radionuclide concentrations.

The DRSPALL results discussed in Appendix PA Section PA-8.3.2 are identical between CRA26_IS and CRA26_FS. These results were not recalculated for CRA26_FS, as the DRSPALL methodology and input parameters remain unchanged. Spallings release volumes for the CRA26_FS are determined by interpolating CRA26_FS repository pressure results from BRAGFLO simulations to the existing DRSPALL results tables.

Table PA-A-7 summarizes spallings release volumes across all scenarios and locations for the CRA26_IS and CRA26_FS analyses. Mean spallings volumes are slightly higher in the CRA26_FS for most scenarios and locations. The fraction of simulations with nonzero spallings releases is also generally higher in the CRA26_FS, reflecting higher repository pressures associated with the expanded FS configuration. In contrast, the mean of nonzero spallings release volumes is generally similar between the CRA26_IS and CRA26_FS, with only minor variations across scenarios and locations.

Figure PA-A-37 and Figure PA-A-38 illustrate nonzero spallings release volumes by scenario and by location, respectively, highlighting variability across vectors and the influence of repository

pressure on release behavior. Figure PA-A-39 shows spallings release concentrations from closure to 10,000 years. Radionuclide concentrations are calculated using the PRECCDFGF code from EPAUNI output as the volume-weighted average concentration across all contact-handled transuranic (CH-TRU) waste streams. Although total inventory activity expressed in EPA Units is similar between the CRA26_IS and CRA26_FS, the increased repository volume in the CRA26_FS (REFCON:VREPOS) results in lower repository-volume–based spallings concentrations.

Table PA-A-7. Spallings Volume Summary for Replicate 1

Scenario	Location	Mean Spallings Volume (m^3) CRA26_IS	Mean Spallings Volume (m^3) CRA26_FS	Fraction of Sim. with Nonzero Releases CRA26_IS	Fraction of Sim. with Nonzero Releases CRA26_FS	Mean of Non-Zero Spallings Releases (m^3) CRA26_IS	Mean of Non-Zero Spallings Releases (m^3) CRA26_FS
S1-DBR	**All**	**0.24**	**0.26**	**11.54%**	**13.96%**	**2.06**	**1.85**
S1-DBR	L	0.28	0.29	13.33%	15.83%	2.13	1.84
S1-DBR	M	0.28	0.29	13.33%	15.83%	2.12	1.84
S1-DBR	U	0.27	0.28	12.83%	14.50%	2.09	1.94
S1-DBR	O	0.12	0.17	6.67%	9.67%	1.75	1.77
S2-DBR	**All**	**0.41**	**0.42**	**34.80%**	**34.30%**	**1.18**	**1.22**
S2-DBR	L	0.60	0.57	50.60%	48.80%	1.18	1.17
S2-DBR	M	0.59	0.57	50.60%	48.80%	1.17	1.16
S2-DBR	U	0.33	0.36	26.60%	26.20%	1.26	1.38
S2-DBR	O	0.12	0.18	11.40%	13.40%	1.08	1.33
S3-DBR	**All**	**0.38**	**0.40**	**34.75%**	**34.90%**	**1.10**	**1.15**
S3-DBR	L	0.51	0.49	49.20%	48.20%	1.04	1.01
S3-DBR	M	0.51	0.49	49.20%	47.80%	1.04	1.02
S3-DBR	U	0.36	0.40	27.60%	28.40%	1.29	1.42
S3-DBR	O	0.15	0.23	13.00%	15.20%	1.13	1.51
S4-DBR	**All**	**0.20**	**0.24**	**13.15%**	**15.70%**	**1.52**	**1.50**
S4-DBR	L	0.23	0.25	15.00%	17.40%	1.54	1.42
S4-DBR	M	0.23	0.24	15.00%	17.40%	1.53	1.41
S4-DBR	U	0.23	0.28	14.80%	16.60%	1.57	1.68
S4-DBR	O	0.11	0.17	7.80%	11.40%	1.36	1.50
S5-DBR	**All**	**0.28**	**0.33**	**15.90%**	**19.15%**	**1.73**	**1.73**
S5-DBR	L	0.32	0.36	18.20%	21.00%	1.76	1.70
S5-DBR	M	0.32	0.36	18.20%	21.00%	1.76	1.69
S5-DBR	U	0.32	0.38	18.00%	20.80%	1.76	1.83
S5-DBR	O	0.14	0.23	9.20%	13.80%	1.57	1.66
All Scenarios	**All Locations**	**0.30**	**0.33**	**21.63%**	**23.23%**	**1.38**	**1.41**
All	**L**	0.38	0.39	28.65%	29.69%	1.34	1.30
All	**M**	0.38	0.39	28.65%	29.62%	1.34	1.30
All	**U**	0.30	0.34	19.69%	21.04%	1.53	1.61
All	**O**	0.13	0.19	9.50%	12.58%	1.34	1.55

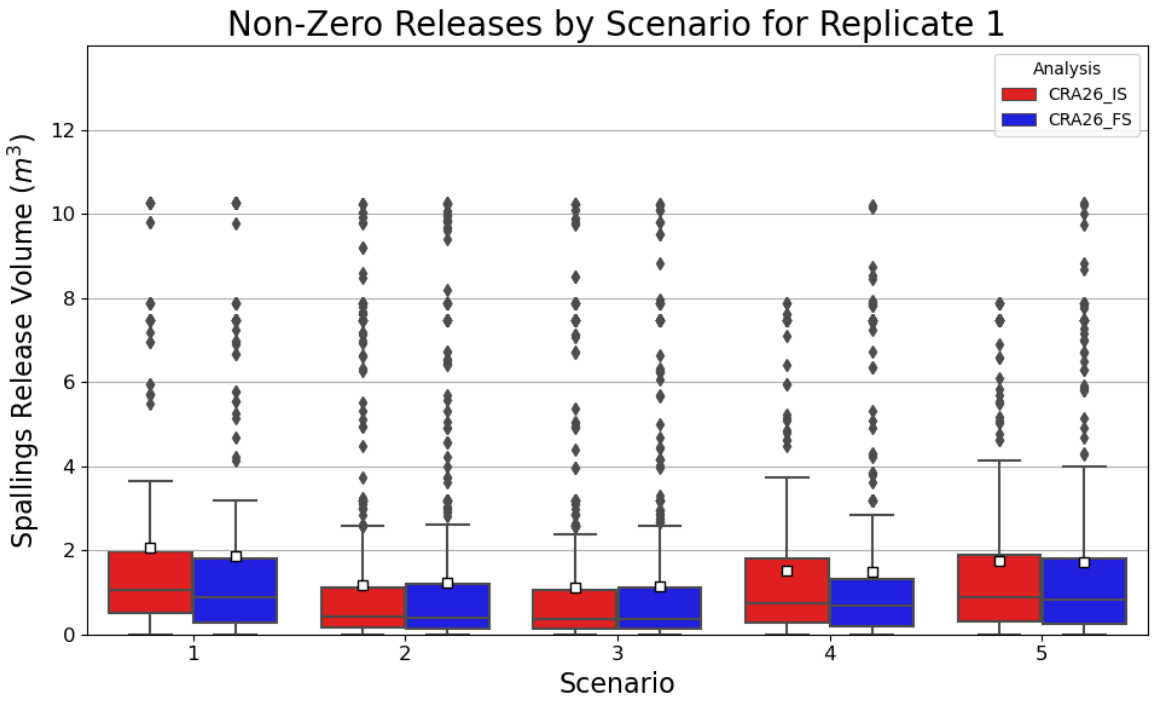


Figure PA-A-37. Non-Zero Spallings Release Volume by Scenario[2]

[2] Boxplots are used to facilitate visualizing and comparing distributions of results. The convention used in this section is that the "box" bottom and top edges indicate the 25th and 75th percentiles (the interquartile range, or IQR), the box interior line indicates the 50th percentile (median), and the square marker indicates the mean. The "whiskers" (the extended vertical lines with horizontal bars) extend to 1.5 times the IQR from the box edges, and the diamond markers exterior to the whiskers are discrete outliers (i.e., points beyond this range).

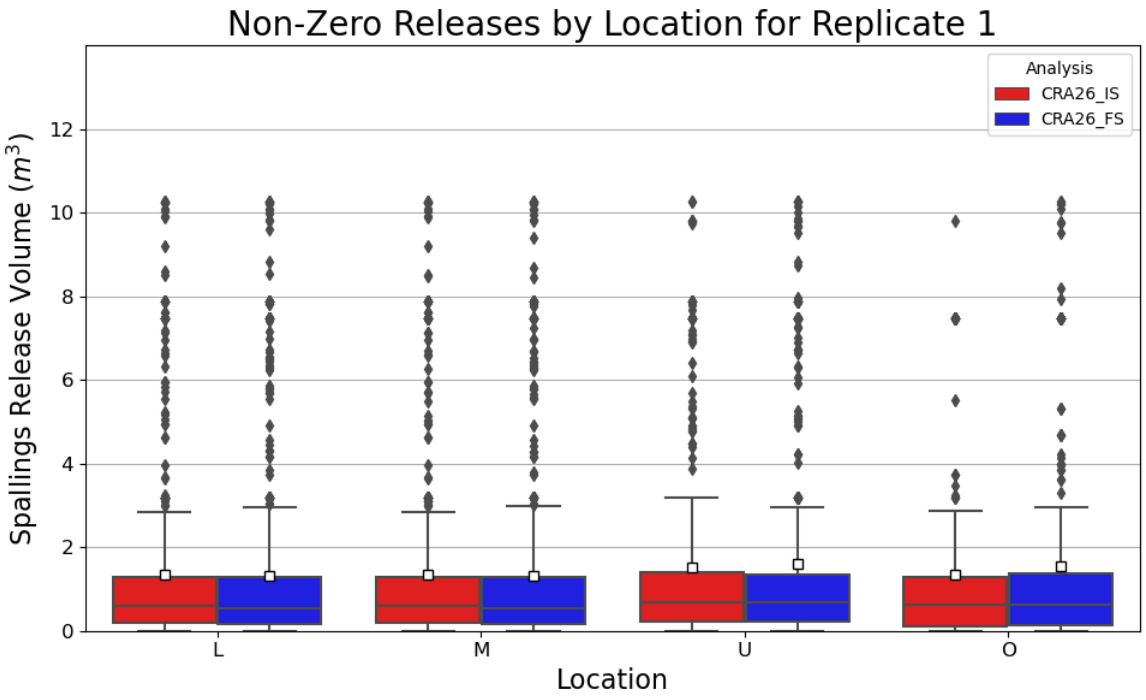


Figure PA-A-38. Non-Zero Spallings Release Volume by Location

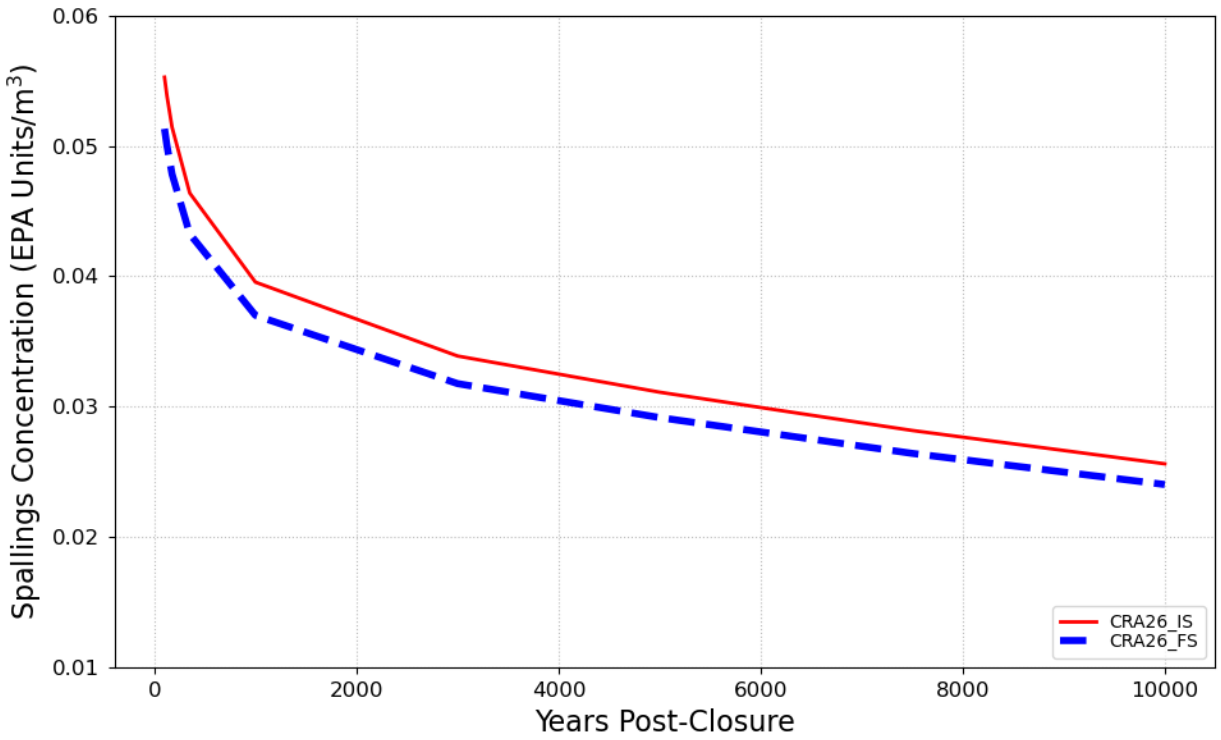


Figure PA-A-39. Spallings Release Concentration from Closure to 10,000 Years

PA-A-5.3.3 Direct Brine Releases

A DBR occurs when brine migrates upward through an intrusion borehole under conditions of sufficient repository brine pressure and saturation. A DBR is influenced by repository pressure, brine saturation, and the location of the intrusion borehole within the repository. This section presents DBR volume results calculated by BRAGFLO for the FS repository configuration and compares them to results for the IS repository.

Table PA-A-8 summarizes DBR volume statistics across all scenarios and intrusion locations for the CRA26_IS and CRA26_FS analyses. Mean DBR volumes are higher in the CRA26_FS than in the CRA26_IS for all scenarios and locations. The fraction of simulations with nonzero DBR volumes is also higher in the CRA26_FS, reflecting increased brine availability associated with higher brine pressures and saturations in the FS repository. Mean nonzero DBR volumes are generally higher in the CRA26_FS, with the largest increases observed for intrusions at the lower (“L”) location.

Figure PA-A-40 and Figure PA-A-41 illustrate DBR volume frequencies and nonzero DBR volumes, respectively, for all intrusion scenarios. Figure PA-A-40 shows an increased frequency of smaller nonzero DBR volumes in the CRA26_FS relative to the CRA26_IS. Figure PA-A-41 shows that while the mean of the nonzero DBR volume distribution is slightly higher in the CRA26_FS, the maximum DBR volumes are lower than those observed in the CRA26_IS, indicating a redistribution of nonzero DBR volumes toward more frequent but generally smaller releases.

Overall, the results indicate that increased brine availability in the CRA26_FS contributes to higher frequencies and mean volumes of DBRs relative to the CRA26_IS. These trends are observed across all intrusion scenarios and locations and demonstrate the influence of the FS repository configuration on DBR release behavior.

Table PA-A-8. DBR Volume Statistics

Intrusion Location	Mean Brine Released (m^3)		Fraction of Simulations with Non-Zero Releases		Mean of Non-Zero Brine Releases (m^3)	
	CRA26_IS	CRA26_FS	CRA26_IS	CRA26_FS	CRA26_IS	CRA26_FS
S1-DBR	**0.30**	**0.53**	**5.04%**	**7.12%**	**6.05**	**7.38**
L	0.78	1.38	9.67%	12.33%	8.11	11.18
M	0.20	0.30	3.67%	5.33%	5.53	5.66
U	0.19	0.31	4.83%	6.33%	3.87	4.82
O	0.05	0.12	2.00%	4.50%	2.28	2.58
S2-DBR	**1.32**	**1.77**	**27.75%**	**33.10%**	**4.77**	**5.34**
L	3.66	4.66	62.40%	68.40%	5.87	6.82
M	1.20	1.73	39.20%	46.80%	3.06	3.70
U	0.33	0.49	6.60%	11.20%	5.06	4.41
O	0.10	0.18	2.80%	6.00%	3.57	3.03
S3-DBR	**0.69**	**1.00**	**22.10%**	**28.40%**	**3.13**	**3.52**
L	1.94	2.67	51.00%	64.00%	3.81	4.17
M	0.52	0.62	27.20%	32.40%	1.91	1.90
U	0.25	0.53	6.80%	10.40%	3.68	5.08
O	0.06	0.18	3.40%	6.80%	1.70	2.67
S4-DBR	**0.68**	**0.93**	**7.75%**	**11.65%**	**8.79**	**7.94**
L	1.76	2.27	15.20%	17.80%	11.55	12.73
M	0.52	0.75	6.80%	12.40%	7.65	6.01
U	0.35	0.51	6.40%	10.40%	5.44	4.87
O	0.10	0.18	2.60%	6.00%	3.84	3.05
S5-DBR	**0.70**	**1.11**	**7.90%**	**11.70%**	**8.88**	**9.45**
L	2.07	2.79	15.20%	19.20%	13.61	14.56
M	0.40	0.81	6.60%	10.80%	6.08	7.46
U	0.28	0.62	6.40%	10.00%	4.32	6.22
O	0.06	0.20	3.40%	6.80%	1.79	2.92
All Scenarios						
L	**1.99**	**2.70**	**29.88%**	**35.42%**	**6.67**	**7.63**
M	**0.55**	**0.82**	**16.19%**	**20.92%**	**3.43**	**3.91**
U	**0.28**	**0.48**	**6.15%**	**9.54%**	**4.48**	**5.07**
O	**0.07**	**0.17**	**2.81%**	**5.96%**	**2.56**	**2.85**
ALL	**0.72**	**1.04**	**13.76%**	**17.96%**	**5.26**	**5.81**

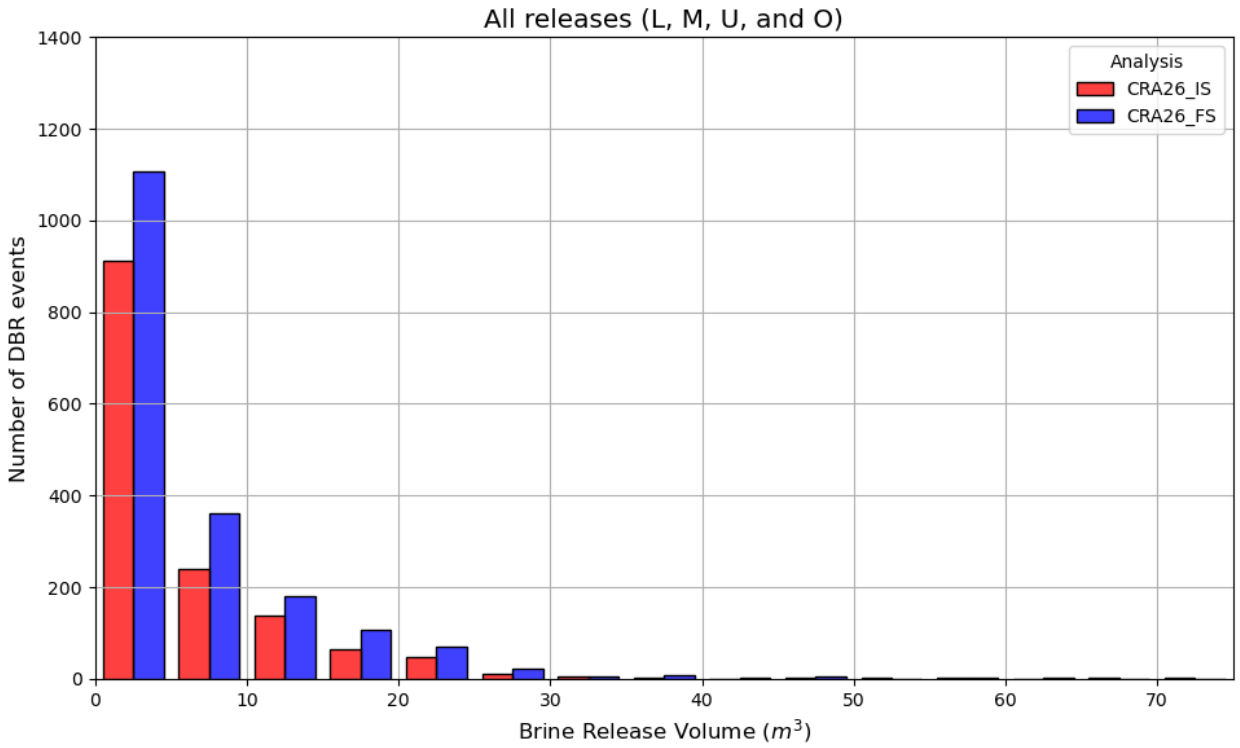


Figure PA-A-40. DBR Volume Frequency, All Intrusions

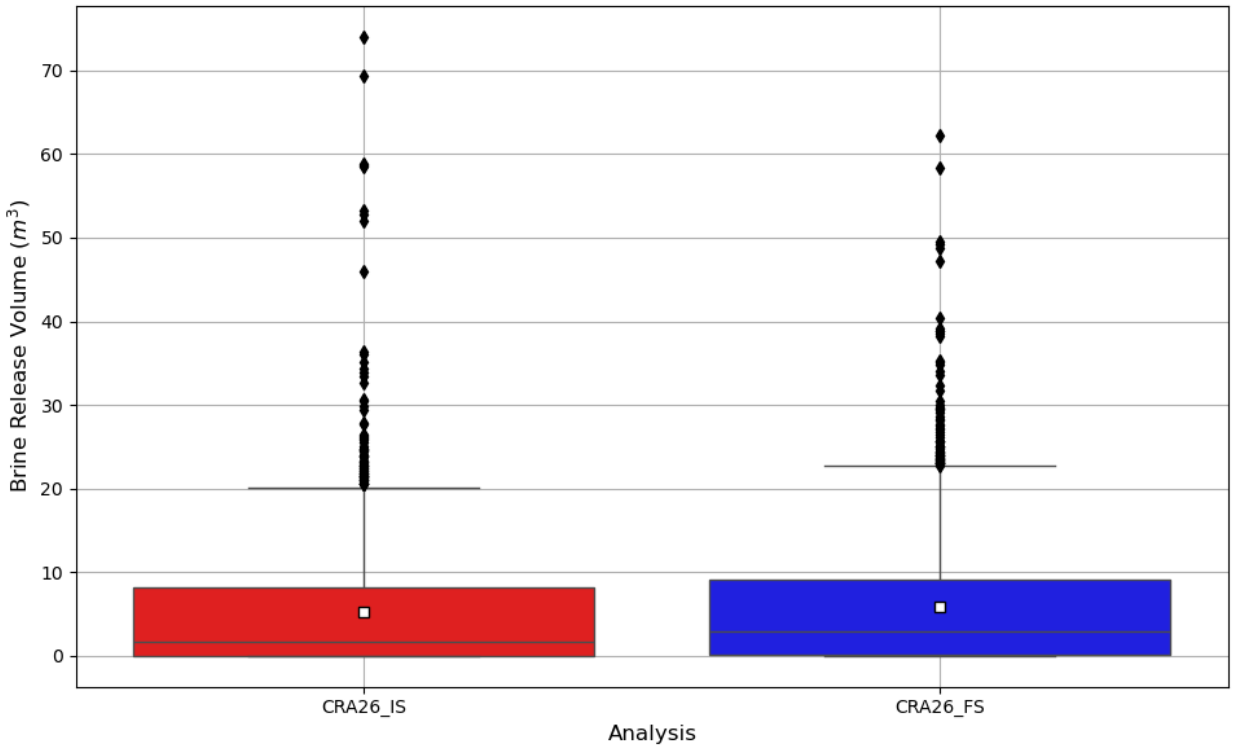


Figure PA-A-41. DBR Volumes, All Non-Zero Releases[2]

PA-A-6.0 Normalized Releases

The radioactive waste disposal regulations of 40 CFR Part 191, Subparts B and C, include containment requirements for radionuclides. Specifically, 40 CFR 191.13 requires that cumulative releases from a disposal system to the accessible environment over 10,000 years not exceed the containment limits specified for the probability levels defined in that section. Releases are expressed in EPA units using the radionuclide-specific release limits provided in Appendix A to Part 191, which serve as normalization factors for calculating total releases. As specified in 40 CFR 194.34, PA results are presented as complementary cumulative distribution functions (CCDFs) of total normalized releases.

Releases from the CRA26_FS PA are influenced by the expanded repository footprint and increased waste inventory. While the larger repository footprint results in a greater number of potential intrusion locations, the lower radionuclide concentrations associated with the FS inventory partially offset the impact of these intrusions on total releases. This section presents results for the four release categories that contribute to total normalized releases—cuttings and cavings, spallings, DBRs, and transport releases, followed by the total normalized releases for the CRA26_FS PA. A comparison between CRA26_FS and CRA26_IS results is also presented.

Normalized releases associated with individual release mechanisms are generally higher for the CRA26_FS than for the CRA26_IS across much of the probability range, with the exception of cuttings and cavings, for which releases are reduced except at very high probabilities. Total normalized releases are dominated by cuttings and cavings at high probabilities and by spallings and DBRs at low probabilities, while contributions from Culebra transport remain comparatively small. The resulting CCDFs of total releases for the CRA26_FS PA remain within the regulatory limits specified in 40 CFR 191.13.

PA-A-6.1 Cuttings and Cavings

Cuttings and cavings releases occur during drilling intrusions when waste material is removed by the drill bit or eroded into the borehole fluid. These releases are influenced by repository dimensions, waste activity concentrations, and the probability of intersecting high-activity waste streams.

Figure PA-A-42 illustrates the mean cuttings and cavings releases, averaged over all three replicates, for the CRA26_FS and CRA26_IS as a function of probability. At probabilities greater than approximately 50 percent, cuttings and cavings releases are higher in the CRA26_FS, reflecting the larger repository footprint and the increased likelihood of intersecting high-activity waste streams. At probabilities below approximately 50 percent, cuttings and cavings releases are lower in the CRA26_FS than in the CRA26_IS, driven primarily by reduced waste activity concentrations in the FS repository.

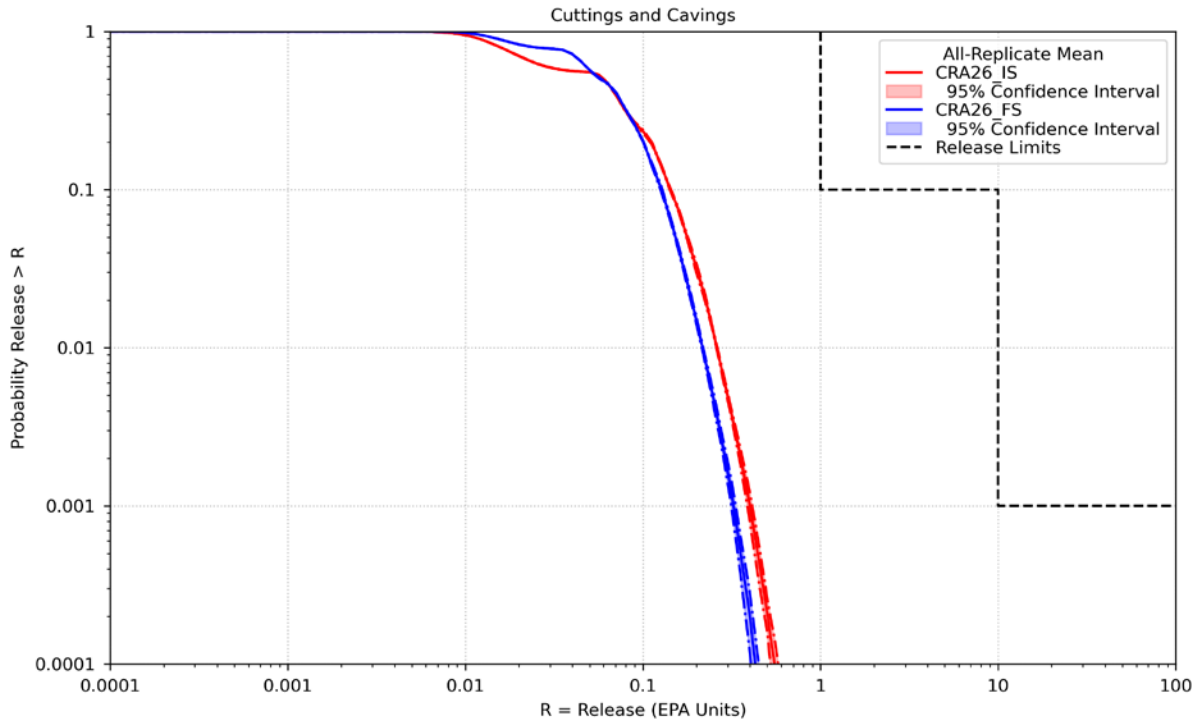


Figure PA-A-42. Overall Mean Cuttings and Cavings Releases

PA-A-6.2 Spallings

Spallings releases occur when repository pressures exceed the hydrostatic pressure of the drilling fluid column during an intrusion event, resulting in the expulsion of waste material from the repository into the borehole. Spallings releases are influenced by repository pressure, brine saturation, and radionuclide concentrations.

Figure PA-A-43 illustrates the mean spallings releases, averaged over all three replicates, for the CRA26_FS and CRA26_IS as a function of probability. Spallings releases are nearly identical between the CRA26_FS and CRA26_IS across the probability range. Minor differences are observed at lower probabilities, with slightly higher mean releases in the CRA26_FS, attributed to marginal increases in repository pressure and brine saturation in the FS repository. At higher probabilities, spallings releases remain consistent between the CRA26_FS and CRA26_IS.

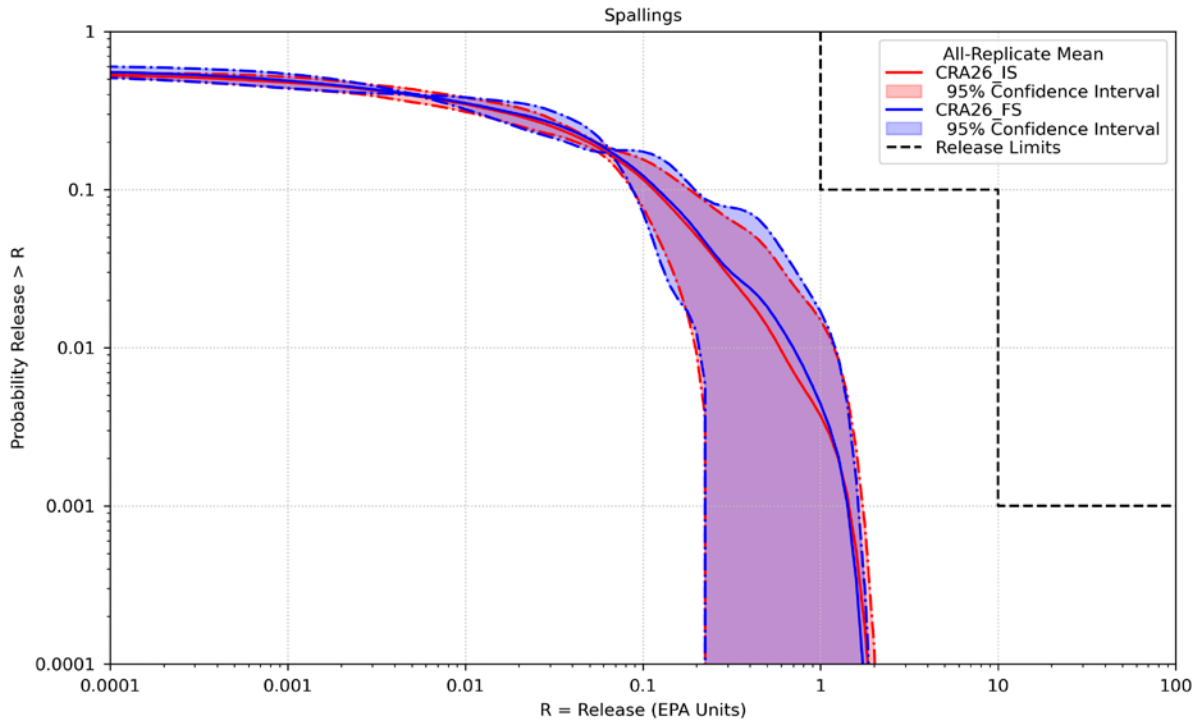


Figure PA-A-43. Overall Mean Spallings Releases

PA-A-6.3 Direct Brine

A DBR occurs when brine migrates upward through an intrusion borehole under conditions of sufficient repository brine pressure and saturation. A DBR is influenced by repository pressure, brine saturation, and the location of the intrusion borehole within the repository.

Figure PA-A-44 illustrates the mean DBR releases, averaged over all three replicates, for the CRA26_FS and CRA26_IS as a function of probability. At higher probabilities, DBR releases are greater in the CRA26_FS, reflecting increased brine availability associated with higher brine saturations in the FS repository. At probabilities below approximately 0.002, DBR releases are slightly lower in the CRA26_FS than in the CRA26_IS, attributable to reduced mobile radionuclide concentrations in the FS repository, which reduce the normalized consequence of DBRs.

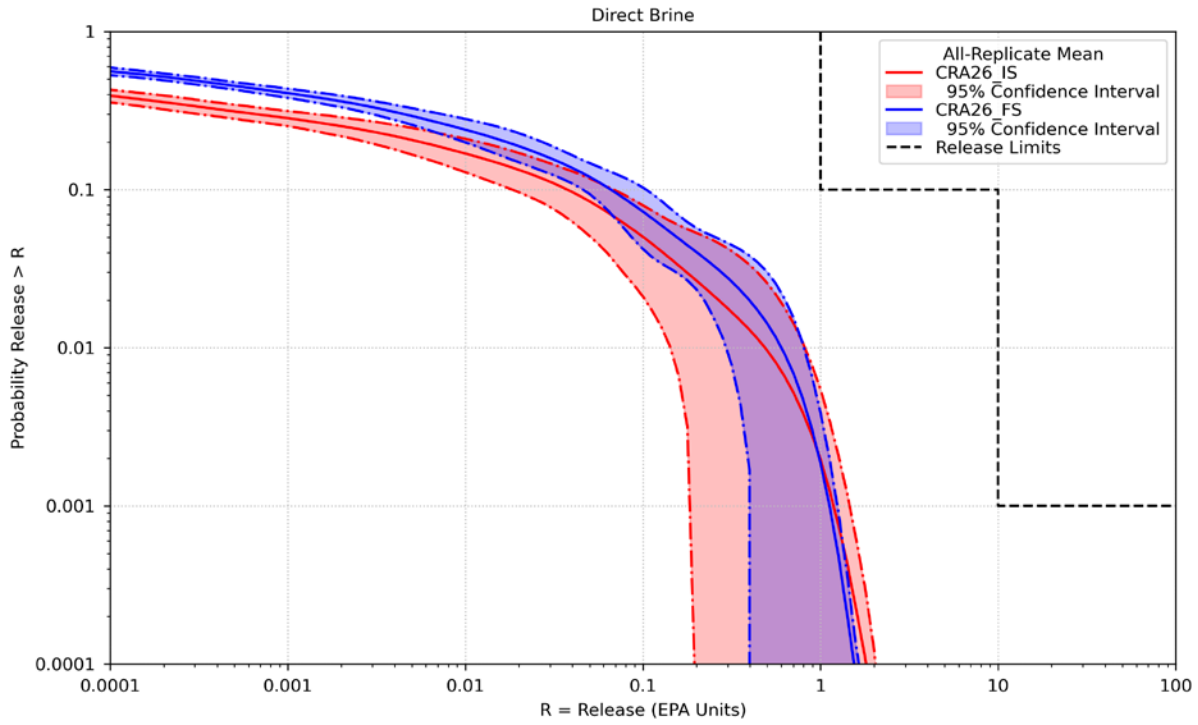


Figure PA-A-44. Overall Mean Direct Brine Releases

PA-A-6.4 Groundwater Transport

Releases through the Culebra occur when radionuclides are transported laterally through the Culebra to the LWB. These releases are influenced by radionuclide concentrations entering the Culebra, transmissivity fields, and radionuclide decay and sorption processes.

Figure PA-A-45 illustrates the mean releases through the Culebra, averaged over all three replicates, for the CRA26_FS and CRA26_IS as a function of probability. Releases for the CRA26_IS remain below the plotting cutoff of 1×10^{-4} EPA Units and therefore do not appear in the figure. In the CRA26_FS, the addition of Culebra release points (CRP 3 and CRP 4) introduces radionuclide transport pathways associated with the westernmost panels (Panels 14 through 19) in the CRA26_FS, resulting in nonzero releases through the Culebra.

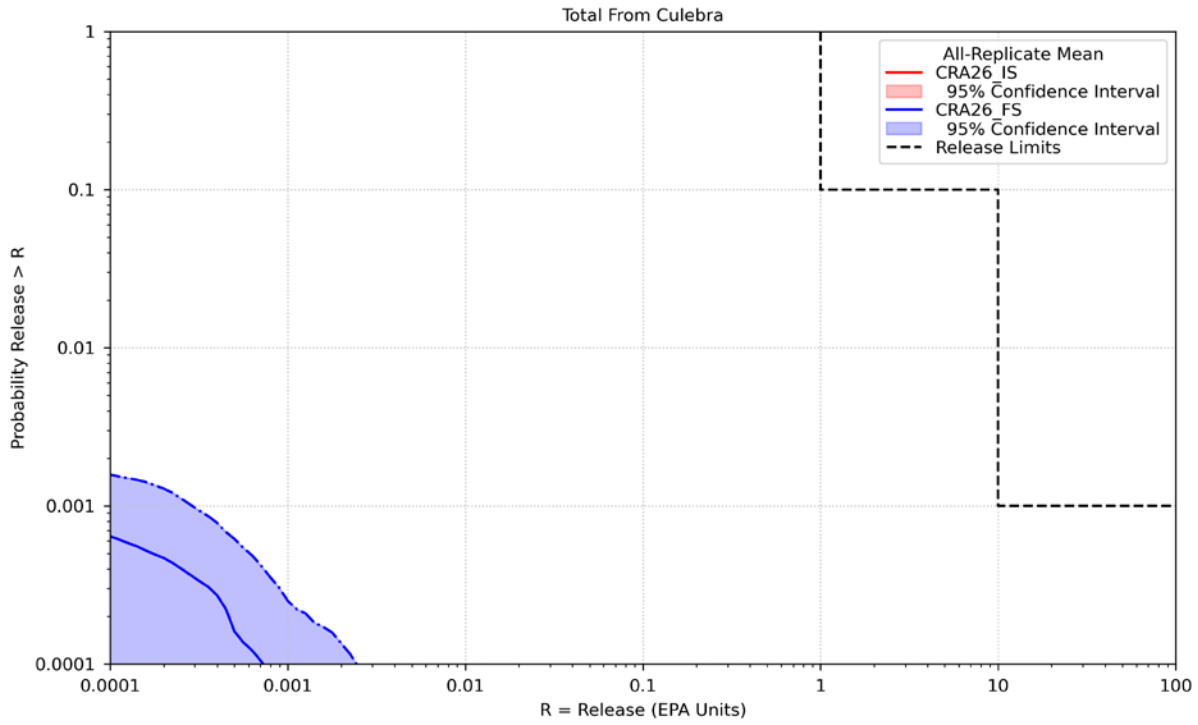


Figure PA-A-45. Overall Mean Releases Through the Culebra

PA-A-6.5 Total Normalized Releases

Total releases account for contributions from all release mechanisms, including cuttings and cavings, spallings, DBRs, and releases through the Culebra. Total releases are expressed in EPA Units and presented as CCDFs to evaluate compliance with the containment requirements of 40 CFR 191.13.

Figures PA-A-46 through PA-A-48 illustrate the CCDFs of total releases for Replicates 1, 2, and 3 of CRA26_FS. Figure PA-A-49 shows the mean release components, averaged over all three replicates, for CRA26_FS, providing insight into the relative contributions of each release mechanism to total releases. Figure PA-A-50 presents the mean total releases for CRA26_FS, averaged over all three replicates, which are compared to CRA26_IS results in Table PA-A-9.

The results indicate that total releases for CRA26_FS are slightly increased compared to CRA26_IS at most probabilities, while remaining well below regulator limits. These differences are primarily driven by increased contributions from spallings and DBRs in CRA26_FS, reflecting the expanded repository footprint and increased brine availability.

The CCDFs of total releases for CRA26_FS remain within the regulatory limits defined in 40 CFR 191.13. Overall, the results demonstrate that the Final State repository configuration performs

similarly to the Interim State configuration in terms of total releases, with only minor differences observed across probabilities.

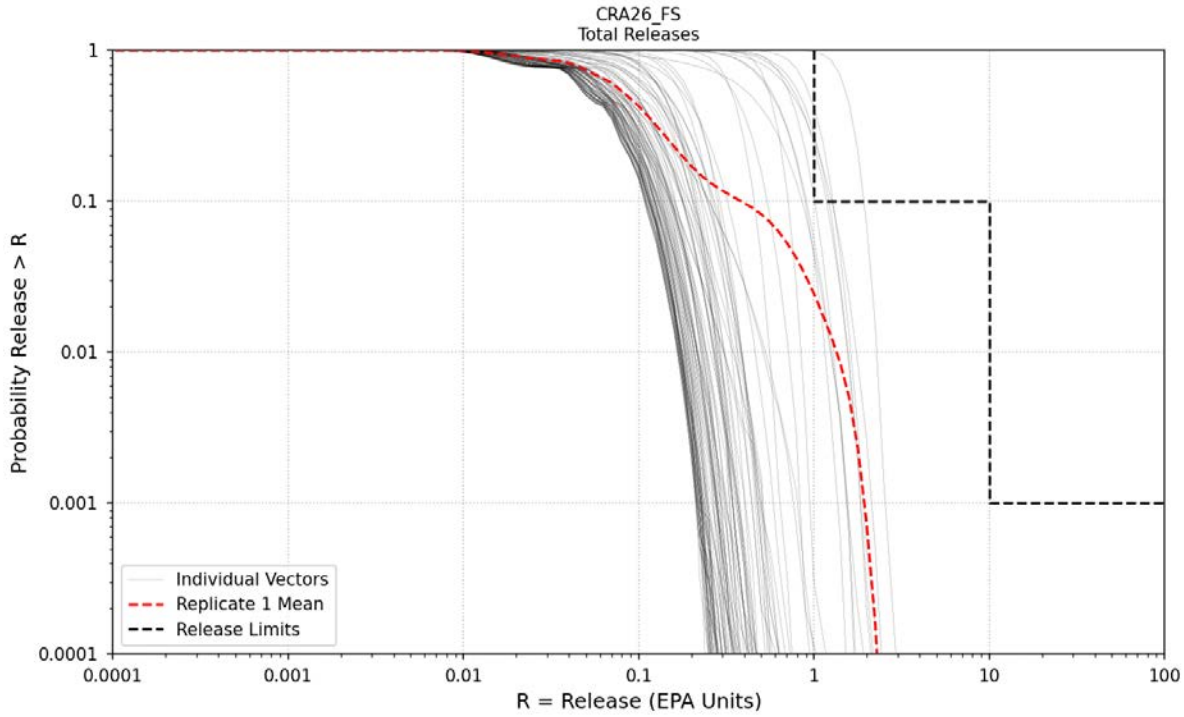


Figure PA-A-46. Total Releases for Replicate 1 of the CRA26_FS

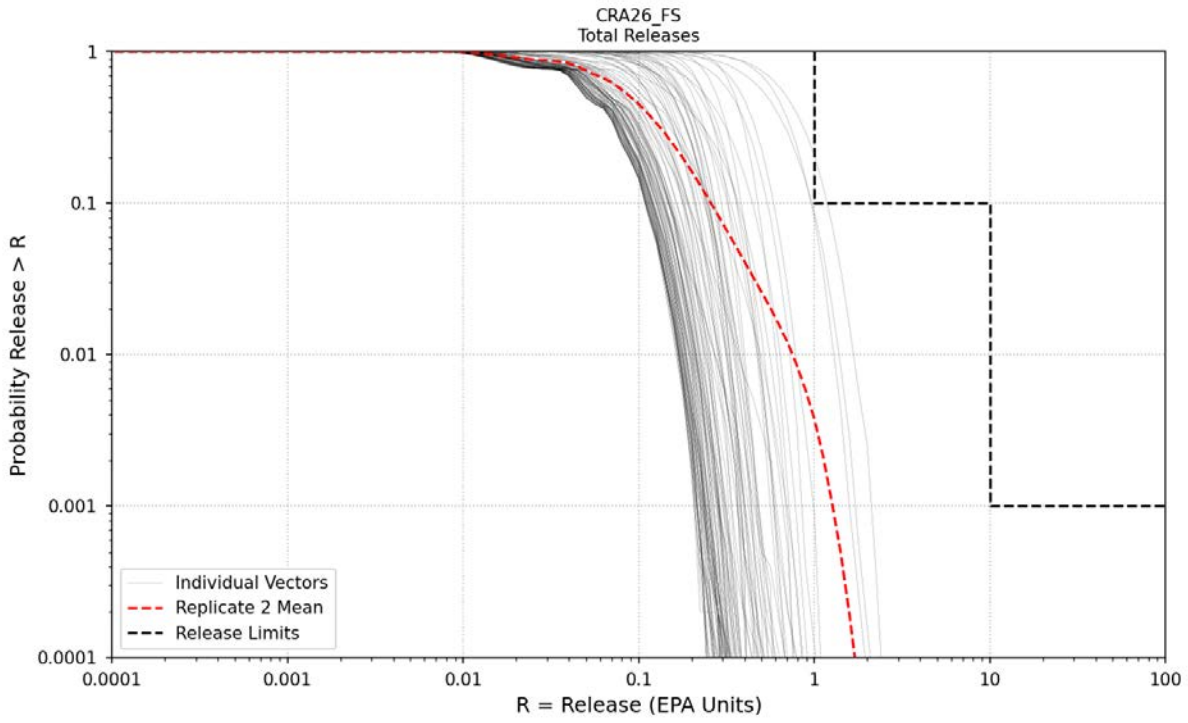


Figure PA-A-47. Total Releases for Replicate 2 of the CRA26_FS

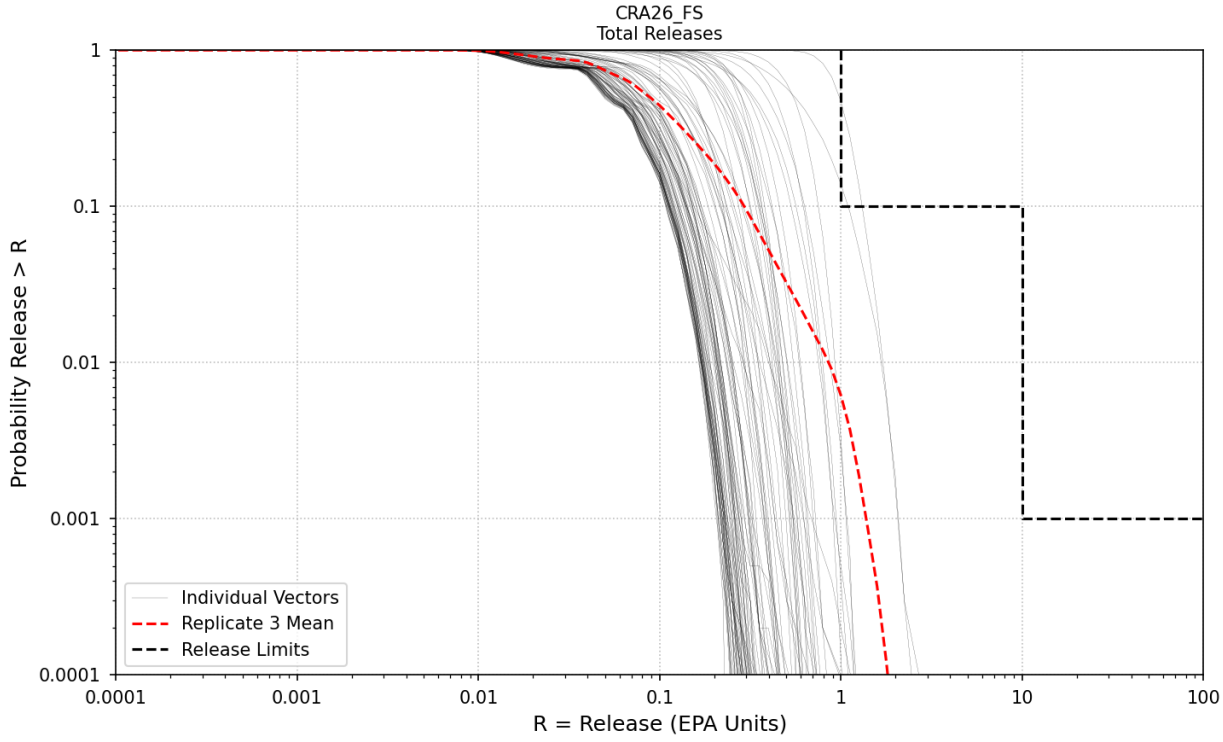


Figure PA-A-48. Total Releases for Replicate 3 of the CRA26_FS

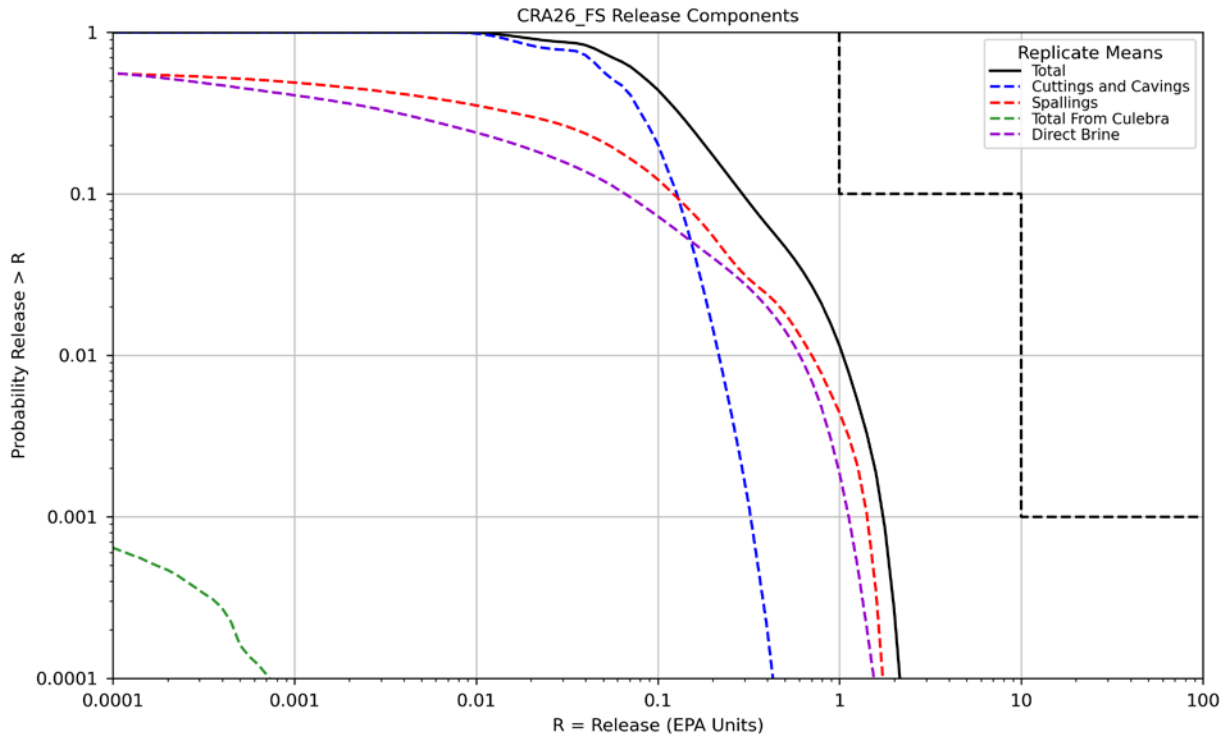


Figure PA-A-49. Overall Mean Release Components for the CRA26_FS

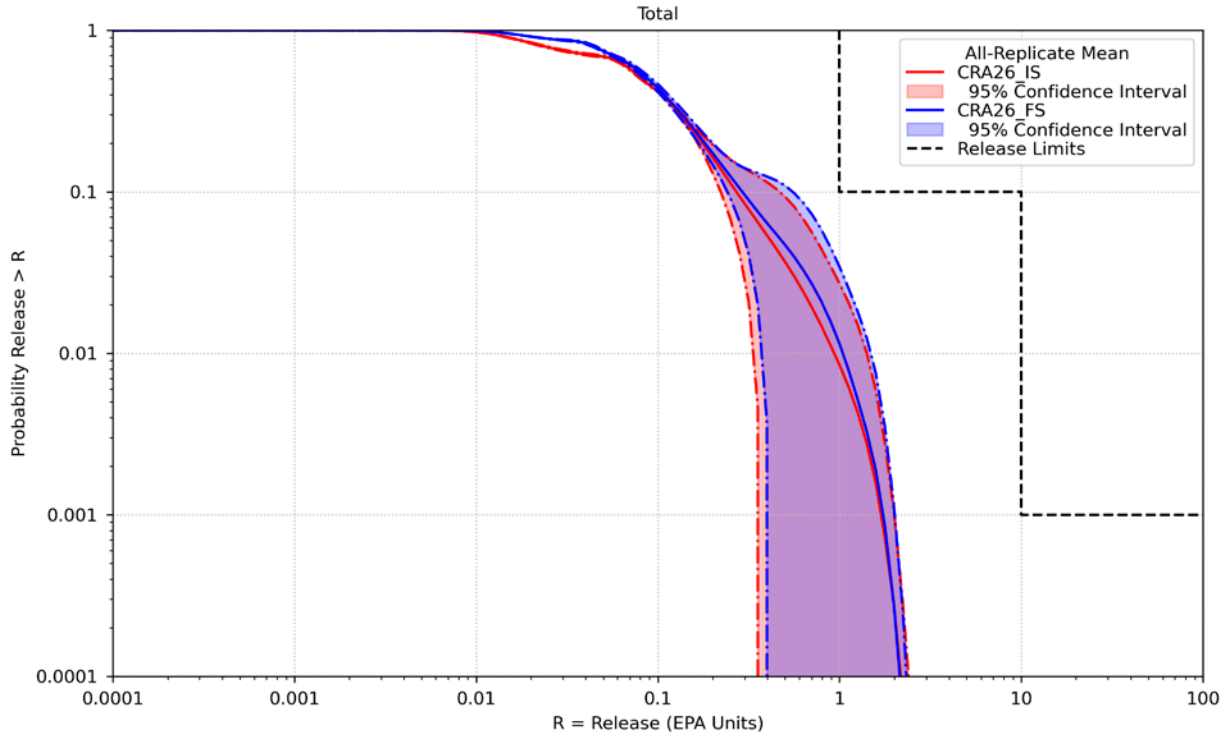


Figure PA-A-50. Overall Mean Total Releases for the CRA26_FS

Table PA-A-9. Statistics on the Overall Mean for Total Releases

Analysis	P(R)>0.1 Lower CI (EPA Units)	P(R)>0.1 Mean (EPA Units)	P(R)>0.1 Upper CI (EPA Units)	P(R)>0.1 Release Limit (EPA Units)	P(R)>0.001 Lower CI (EPA Units)	P(R)>0.001 Mean (EPA Units)	P(R)>0.001 Upper CI (EPA Units)	P(R)>0.001 Release Limit (EPA Units)
CRA26_IS	0.2219	0.2713	0.4679	1	0.3678	1.7121	2.0062	10
CRA26_FS	0.2419	0.2922	0.5516	1	0.4092	1.7489	2.0251	10

PA-A-6.6 Parameter Sensitivity Analysis

A stepwise linear multiple regression analysis was performed to determine the relative sensitivity of the calculated releases to the sampled parameters for CRA26_FS (Zeitler et al. 2025). The sensitivity analysis identifies the parameters contributing most to the variability observed in the mean releases calculated for each vector. The methodology for sensitivity analysis in CRA26_FS remains consistent with that used in CRA26_IS, as described in King et al. (2025).

The dominant parameter contributing to variability in mean total releases across all three replicates is the porosity of the intact Salado halite (S_HALITE:POROSITY). In the CRA26_FS analysis, S_HALITE:POROSITY explains 22–32% of the variability in mean total releases, compared to 18–27% in CRA26_IS. This parameter's influence is attributed to its significant impact on repository pressure and brine saturation, which directly affect spallings and direct brine release volumes.

Other notable parameters include:

- BOREHOLE:TAUFAIL: Representing waste shear strength, this parameter is the second most influential across both analyses, explaining 5–15% of variability in CRA26_FS and 6–13% in CRA26_IS. Its importance is tied to its role in cuttings and cavings releases.
- SPALLMOD:PARTDIAM: Particle diameter for spallings, contributed 3–13% of variability in CRA26_FS and 5–17% in CRA26_IS. This parameter directly impacts spallings releases, which contribute significantly to total releases.
- CASTILER:PRESSURE: Initial brine pore pressure in the Castile reservoir contributes 4–6% of variability in CRA26_FS and 3–5% in CRA26_IS, highlighting its role in influencing repository pressure and brine flow behavior.

The sensitivity analysis results for CRA26_FS align closely with those for CRA26_IS, underscoring the dominant role of repository pressure and brine saturation dynamics, driven by

S_HALITE:POROSITY, as well as the influence of SPALLMOD:PARTDIAM and BOREHOLE:TAUFAIL. These findings are consistent across all three replicates.

Detailed sensitivity analysis results, including stepwise ranked regression analyses for mean total releases and comparison with the CRA26_IS, are presented in Zeitler et al. (2025).

PA-A-7.0 References

(*Indicates a reference that has not been previously submitted.)

Brunell, S. 2025. Update to CRA-2026 PA Input Parameters Due to Revised WIPP Repository Dimensions. Carlsbad, NM: Sandia National Laboratories. EIMS-0004799007. *

Brunell, S., B. Day, P. Docherty, D. Kicker, S. Kim, S. King, J. Long, J. Wilgus, and T. Zeitler. 2025. Summary Report for the 2026 Compliance Recertification Application Performance Assessment: Interim State Repository. Rev. 0. Carlsbad, NM: Sandia National Laboratories. EIMS-0005119328 *

Day, B. 2025. BRAGFLO Grid Development for CRA-2026. Carlsbad, NM: Sandia National Laboratories. EIMS-0004447000. *

Domski, P. 2025. Th(IV), Np(V), and Am(III) Baseline Solubilities for the 2026 WIPP Compliance Recertification Application Performance Assessment Final-State Analysis (CRA26_FS). Carlsbad, NM: Sandia National Laboratories. EIMS-0004800933. *

Feng, M. and D.C. Kicker. 2025. Input Parameter Report for the 2026 Compliance Recertification Application Performance Assessment: Final State Repository (CRA-2026 FS) Rev. 2. Carlsbad, NM: Sandia National Laboratories. EIMS-0005148804. *

Hansen, C., S. Brunell, B. Day, S. King, and J. Wilgus. 2025. Analysis Plan for the 2026 WIPP Compliance Recertification Application Performance Assessment. Carlsbad, NM: Sandia National Laboratories. AP-214. *

Kicker, D. 2025a. Analysis Report for Radionuclide Inventory Screening in the 2026 Compliance Recertification Application Performance Assessment: Final State Repository. Revision 0. Carlsbad, NM: Sandia National Laboratories. EIMS-0004799526. *

Kicker, D. 2025b. Analysis Report for Radionuclide Inventory Screening in the 2026 Compliance Recertification Application Performance Assessment: Interim State Repository. Revision 0. Carlsbad, NM: Sandia National Laboratories. EIMS-0004832100. *

King, S., S. Brunell, and T. Zeitler. 2025. Analysis Report for Normalized Releases in the 2026 Compliance Recertification Application Performance Assessment: Interim State Repository. Carlsbad, NM: Sandia National Laboratories. EIMS-0005040307. *

Long, J. 2025. Computational Code Execution and File Management for the 2026 Compliance Recertification Application Performance Assessment: Final State Repository (CRA-2026 FS). Rev. 0. Carlsbad, NM: Sandia National Laboratories. EIMS-0004899943. *

Mariner, P. 2025. CRA26_FS Updates to the WIPP Humic Colloids Models for An(III) and An(IV). Carlsbad, NM: Sandia National Laboratories. EIMS-0004800929. *

U.S. Congress. 1996. Public Law 102-579. Waste Isolation Pilot Plant Land Withdrawal Act of 1992, as amended by Public Law 104-201, 1996. Washington, DC. ERMS 239105.

Van Soest, G.D. 2025a. Full Repository Performance Assessment Inventory Report – 2024. Revision 0. Carlsbad, NM: Los Alamos National Laboratory. INV-FPA-24. *

Ward, A. 2025. Performance Assessment Inventory for Analysis of a 12-Panel Repository Configuration. Letter to Bill McInroy. March 18, 2025. Carlsbad, NM: Department of Energy Carlsbad Field Office. CBFO:ERCD:AW:RS:25-0197. *

Wilgus, J., and S. Brunell. 2025. Re-Calculation of the Location of Culebra Release Point 2 for Use in WIPP PA. Revision 1. Carlsbad, NM: Sandia National Laboratories. EIMS-0004818700.

Wilgus, J., and J. Bethune. 2025. Analysis Report for Culebra Flow and Transport in the 2026 Compliance Recertification Application Performance Assessment. Carlsbad, NM: Sandia National Laboratories. EIMS-0005101531. *

Zeitler, T.R., S. Brunell, B. Day, P. Docherty, D. Kicker, S. Kim, S. King, J. Long, and J. Wilgus. 2025. Analysis Report for the 2026 Compliance Recertification Application Performance Assessment: Final State Repository. Revision 0. Carlsbad, NM: Sandia National Laboratories. EIMS-0005119323. *